

2004

# Is MWP 1A Real and Could It have Originated in the Northern Hemisphere in Response to Bolling Warming

Sean D. Birkel

Follow this and additional works at: <http://digitalcommons.library.umaine.edu/etd>

 Part of the [Climate Commons](#), and the [Glaciology Commons](#)

---

## Recommended Citation

Birkel, Sean D., "Is MWP 1A Real and Could It have Originated in the Northern Hemisphere in Response to Bolling Warming" (2004). *Electronic Theses and Dissertations*. 628.  
<http://digitalcommons.library.umaine.edu/etd/628>

This Open-Access Thesis is brought to you for free and open access by DigitalCommons@UMaine. It has been accepted for inclusion in Electronic Theses and Dissertations by an authorized administrator of DigitalCommons@UMaine.

**IS MWP 1A REAL AND COULD IT HAVE ORIGINATED IN THE  
NORTHERN HEMISPHERE IN RESPONSE TO  
BÖLLING WARMING?**

By

Sean D. Birkel

B.S. University of Maine, 2002

A THESIS

Submitted in Partial Fulfillment of the  
Requirements for the Degree of  
Master of Science  
(in Quaternary and Climate Studies)

The Graduate School

The University of Maine

December, 2004

Advisory Committee:

George H. Denton, Libra Professor of Earth Sciences, Advisor

Brenda L. Hall, Assistant Research Professor of Earth Sciences

James L. Fastook, Professor of Computer Science

**IS MWP 1A REAL AND COULD IT HAVE ORIGINATED IN THE  
NORTHERN HEMISPHERE IN RESPONSE TO  
BÖLLING WARMING?**

By Sean D. Birkel

Thesis Advisor: Dr. George H. Denton

An Abstract of the Thesis Presented  
in Partial Fulfillment of the Requirements for the  
Degree of Master of Science  
(in Quaternary and Climate Studies)  
December, 2004

Meltwater Pulse 1A (MWP 1A) is thought to have encompassed an abrupt rise in sea-level of 19 – 24 m *ca.* 14,000 calendar years B.P. The postulated rate of sea-level rise during the event was 24 – 50 mm/yr. In contrast, the average rate of change during the overall glacial termination was 13 mm/yr. Although MWP 1A is commonly accepted at face value, a compilation of all basic data points casts doubts on its validity.

The Laurentide Ice Sheet (LIS) is commonly cited as the source of MWP 1A. Accelerated discharge of freshwater from the ice sheet could have weakened the formation of North Atlantic deep water. However, with the exception of sea-water freshening observed in cores from the Gulf of Mexico and Bermuda Rise, there is little geologic evidence to support a pulse from the LIS during the time of MWP 1A. An alternative suggestion is that MWP 1A originated in Antarctica. One possibility is that a meltwater pulse could have been derived by exploding ice shelves followed by accelerated seaward discharge from ice streams. However, Antarctica contributed at

most 18 m, but probably less than 14 m to total LGM sea-level lowering. Furthermore, West Antarctica, which contained two-thirds of the excess Antarctic ice volume at the LGM, did not undergo substantial deglaciation until mid to late-Holocene time, well after MWP 1A.

The University of Maine Ice Sheet Model (UMISM) was employed to explore the physical plausibility of MWP 1A coming from the LIS. A GISP2 record of temperature was used as input to drive mass-balance calculations. However, the extremely low temperatures in the climate signal prevented the model from generating a realistic ice sheet. Based on similarities to sea-level reconstructions, the EPICA Dome C ice core record was then used as an alternate proxy for climate. Results indicate that a 10.5 m meltwater pulse is possible in response to climatic warming at the beginning of the Bölling-Alleröd interstadial. However, in order to achieve this result, it was necessary to superimpose on the EPICA forcing a modern climate regime over the ice sheet for 300 model years.

Thus both geological and glaciological results cast serious doubts on the existence of MWP 1A. Even if the constraining sea-level data are interpreted as permitting such a pulse, the glaciological model input must be stimulated by artificial warming superimposed on an Antarctic signal to produce both the correct termination and the postulated magnitude and timing of MWP 1A.



## ACKNOWLEDGMENTS

I would like to thank Dr. George H. Denton (the “Godfather”) for the opportunities he has given me and also for his guidance and inspiration. It has been an honor to work with him. I extend my appreciation to Dr. James L. Fastook for his patience in answering perpetual questions about the University of Maine Ice Sheet Model. I thank Dr. Brenda Hall for giving me the opportunity to work as a field assistant in the Dry Valleys, Antarctica. There are few places on Earth so bizarre and barren, yet so truly wild and beautiful.

I thank the Climate Change Institute and the Jordan Planetarium for financial support.

I am grateful for my family for their undying support and patience. Special thanks go to Mellissia. Without her, I’d be lost.

## TABLE OF CONTENTS

ACKNOWLEDGMENTS.....	ii
LIST OF FIGURES.....	v
Chapter	
1. INTRODUCTION.....	1
2. GEOLOGICAL EVIDENCE.....	3
2.1 Record from Barbados.....	3
2.2 Record from Tahiti.....	7
2.3 Record from the Sunda Shelf.....	10
2.4 Records from other Locations.....	14
3. PREVIOUS INTERPRETATIONS OF MELTWATER PULSE 1A.....	18
3.1 Did MWP 1A originate in the Northern Hemisphere?.....	18
3.2 Did MWP 1A originate in the Southern Hemisphere?.....	21
4. METHODS.....	26
5. RESULTS.....	30
5.1 Experiment 1.....	30
5.2 Discussion.....	42
5.3 Experiment 2.....	49
5.4 Discussion.....	53
6. CONCLUSIONS.....	65
REFERENCES.....	67
APPENDIX A.....	72

APPENDIX B.....75  
BIOGRAPHY OF THE AUTHOR.....78

## LIST OF FIGURES

Figure 1.	A world map showing approximate LGM ice distribution and locations where a MWP 1A signal has been identified.....	4
Figure 2.	Stratigraphic description for the nine longest cores recovered from Barbados.....	5
Figure 3.	Barbados sea-level reconstructions derived from <sup>14</sup> C and U-Th data.....	6
Figure 4.	The Tahiti sea-level reconstruction derived from U-Th data.....	8
Figure 5.	Stratigraphic description for cores P6 and P7 from Tahiti.....	9
Figure 6.	The Sunda Shelf sea-level reconstruction.....	11
Figure 7.	Sunda Shelf stratigraphy.....	13
Figure 8.	Caribbean deglacial sea-level reconstruction.....	15
Figure 9.	Sea level data from Barbados, Tahiti, Huon Peninsula, Sunda Shelf and the Bonaparte Gulf.....	17
Figure 10.	Deglacial chronology of grounded ice in the Ross Sea region.....	25
Figure 11.	Northern and Southern Hemisphere ice-core chronologies.....	27
Figure 12.	The GISP2 record formatted for the UMISM. Mean annual temperatures are derived from oxygen isotope data.....	29
Figure 13.	Ice sheet generated by using the GISP2 record as a proxy for mean-annual temperature change.....	31
Figure 14.	The GISP2 temperature record.....	32
Figure 15.	Experiment 1 results.....	34
Figure 16.	Pattern of glaciation evident from paleoclimate indicators.....	37
Figure 17.	Experiment 1 ice-sheet configurations.....	39
Figure 18.	Typical winter configuration of the polar jet stream over the Northern Hemisphere.....	43
Figure 19.	Comparison of paleoclimate records.....	46

Figure 20. The EPICA Dome C (EDC-2 timescale) and scaled GISP2 records.....	48
Figure 21. The EPICA EDC2 record formatted for the UMISM showing from 20,000 to 10,000 ice core years B.P.....	50
Figure 22. Map-plane mass-balance modifications used in Experiment 2.....	51
Figure 23. Experiment 2 LGM ice-sheet configuration.....	52
Figure 24. Experiment 2 LGM ice-sheet configuration with mass-balance adjustments that prevented growth of ice over the Cordilleran.....	54
Figure 25. Experiment 2 results.....	55
Figure 26. Experiment 2 ice-sheet configurations.....	57
Figure 27. Basal water thickness (in meters).....	62
Figure 28. Thickness difference between -15,000 and -14,600 model years.....	64

# 1. INTRODUCTION

Sea-level recovery during the last glacial-interglacial transition may have included two brief periods of rapid rise caused by accelerated melting of ice sheets (Fairbanks 1989). The average rate of rise during the overall glacial termination was 13 mm/yr. In contrast, sea level is postulated to have risen 24-50 mm/yr during the first and most significant period of rapid change, Meltwater Pulse 1A (MWP 1A) (Fairbanks 1989; Bard *et al.* 1990; Chappell and Polach 1991; Blanchon and Shaw 1995; Bard *et al.* 1996; Hanebuth *et al.* 2000). This event is thought to have encompassed a rise in eustatic sea-level of 13.5-24 m within 300-1000 years near the beginning of the Bölling-Alleröd warm interval (*ca.* 14,000 calendar years B.P). A second meltwater pulse (MWP 1B) of less than 10 m magnitude is postulated at the beginning of the Holocene (Fairbanks 1989).

A collapse of some portion of the Laurentide Ice Sheet (LIS) is commonly cited as the cause of MWP 1A (Fairbanks 1989; Bard *et al.* 1990; Bard *et al.* 1996). A pulse of meltwater from the LIS into the North Atlantic could have stopped the production of North Atlantic deep water (NADW), thereby flipping the mode of thermohaline circulation and triggering the Younger Dryas cold reversal (Fairbanks 1989). Glacial meltwater from the LIS could have discharged into the North Atlantic through three primary outlets: Gulf of Mexico, the Gulf of St. Lawrence and Hudson Strait. However, a review of deep-sea oxygen isotopic records shows that only cores from the Gulf of Mexico and the Bermuda Rise have low  $\delta^{18}\text{O}$  values consistent with an influx of freshwater during the time of MWP 1A (Clark *et al.* 1996).

Discharge from the thin southern sector of the LIS into the Gulf of Mexico may not have been sufficient to account for an event postulated to have been the magnitude of MWP 1A. It is therefore possible that MWP originated from a mechanical collapse of the Antarctic Ice Sheet (AIS) into the Southern Ocean (Clark *et al.* 1996). In such a scenario, at least one ocean model predicts a thermohaline response in the North Atlantic sufficient to trigger the Bölling-Alleröd warm pulse (Clark *et al.* 2002; Weaver *et al.* 2003).

Determining whether MWP 1A actually occurred, and if so its source, has important implications for the understanding the last glacial termination. I sought to evaluate one aspect of this problem from a glaciological perspective using the University of Maine Ice Sheet Model (UMISM): Was the LIS capable of producing a meltwater pulse consistent in time and magnitude with that of MWP 1A?

## 2. GEOLOGICAL EVIDENCE

### 2.1 Record from Barbados

The original record to show a meltwater pulse is that from Barbados in the Caribbean Atlantic (Fig. 1) (Fairbanks 1989), where a series of drill cores was collected offshore from a coral reef (Fig. 2). A nearly continuous sequence of *Acropora palmata* deposited during the sea-level rise of the last deglaciation was recovered to a core depth of ~145 m. Monospecific *A. palmata* reef frameworks form in water depths of less than 5 m; therefore, they are sensitive indicators of sea-level change. A sea-level curve (Fig. 3) was constructed based on the stratigraphy and chronology of radiocarbon (Fairbanks 1989) and  $^{234}\text{U}$ - $^{230}\text{Th}$  dated (Bard *et al.* 1990) *A. palmata* coral samples. One complicating factor in using Barbados as a sea-level dipstick is that the island is situated near an active plate margin. A mean linear tectonic uplift rate of 0.34 mm/yr was identified by evaluating the elevations of onshore ridges of *A. Palmata* (Fairbanks and Matthews 1978). After a correction for tectonic uplift, the LGM sea-level lowstand was estimated to have been 121 +/- 5 m below present mean sea level.

According to the Barbados record, sea level rose on the order of 5 mm/yr between 19,000 and 14,700 calendar years B.P. (17,000 and 12,500  $^{14}\text{C}$  years B.P.) (Fairbanks 1989; Bard *et al.* 1990). This initial phase of gradual deglaciation was terminated by an abrupt rise in sea level (termed a meltwater pulse) of 24 m in less than 1000 years. Meltwater Pulse 1A here unfortunately is only identified by data points that bracket a hiatus between 14,700 +/- 100 and 13,800 +/- 140 calendar years B.P (12,500 +/- 200  $^{14}\text{C}$



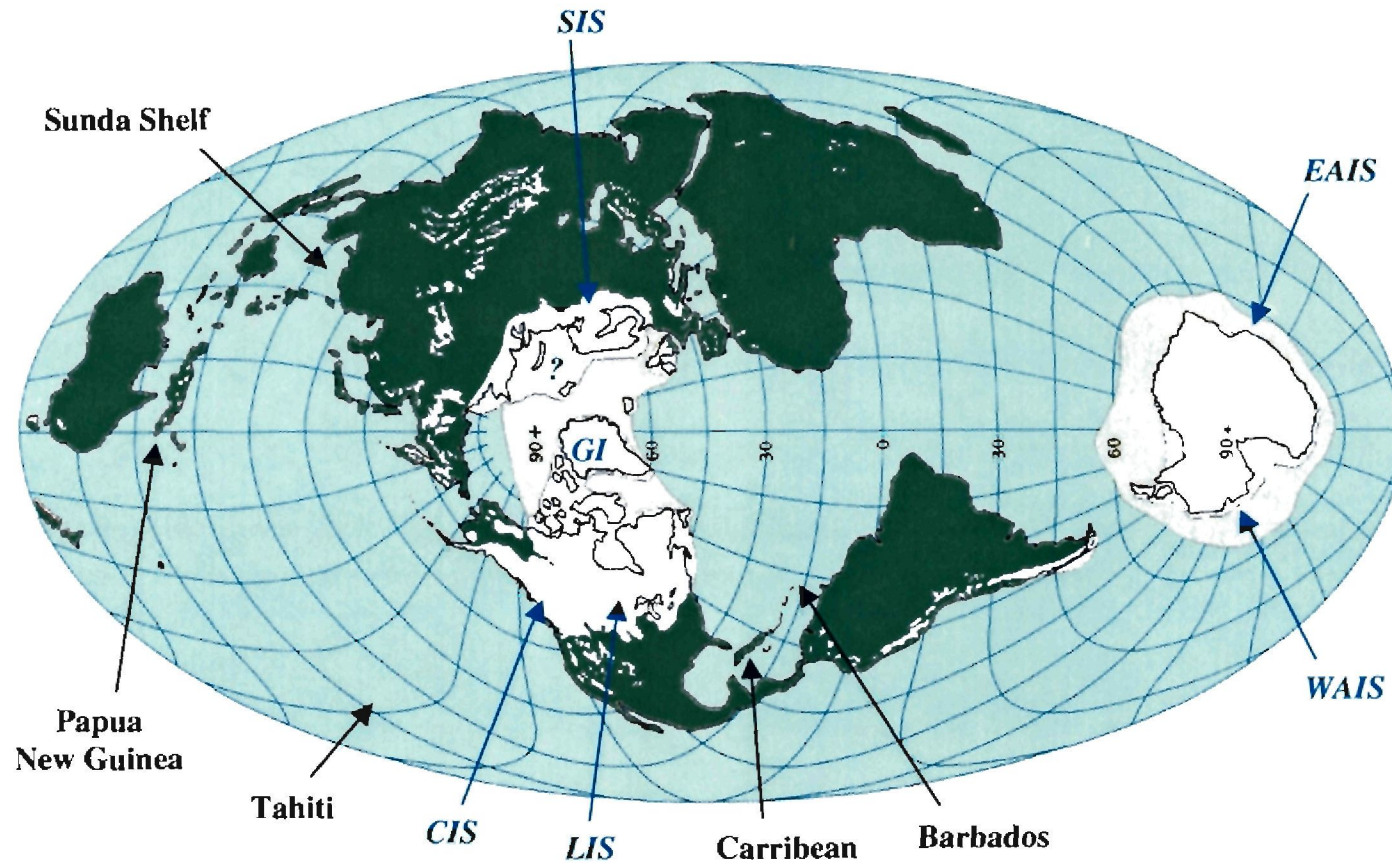


**Fig. 1.** A world map showing approximate LGM ice distribution and locations where a MWP 1A signal has been identified. Cordilleran Ice Sheet (CIS); Laurentide Ice Sheet (LIS); Greenland Ice Sheet (GIS); Scandinavian Ice Sheet (SIS); East Antarctic Ice Sheet (EAIS); West Antarctic Ice Sheet (WAIS); the question mark indicates a possible ice sheet over the Barrents Sea region. Base map modified from Broecker and Denton (1990).

# Barbados Offshore Drilling Program

Research Vessel N.U.S.C. Ranger Cruise 88-13 18/November/88 - 6/December/88

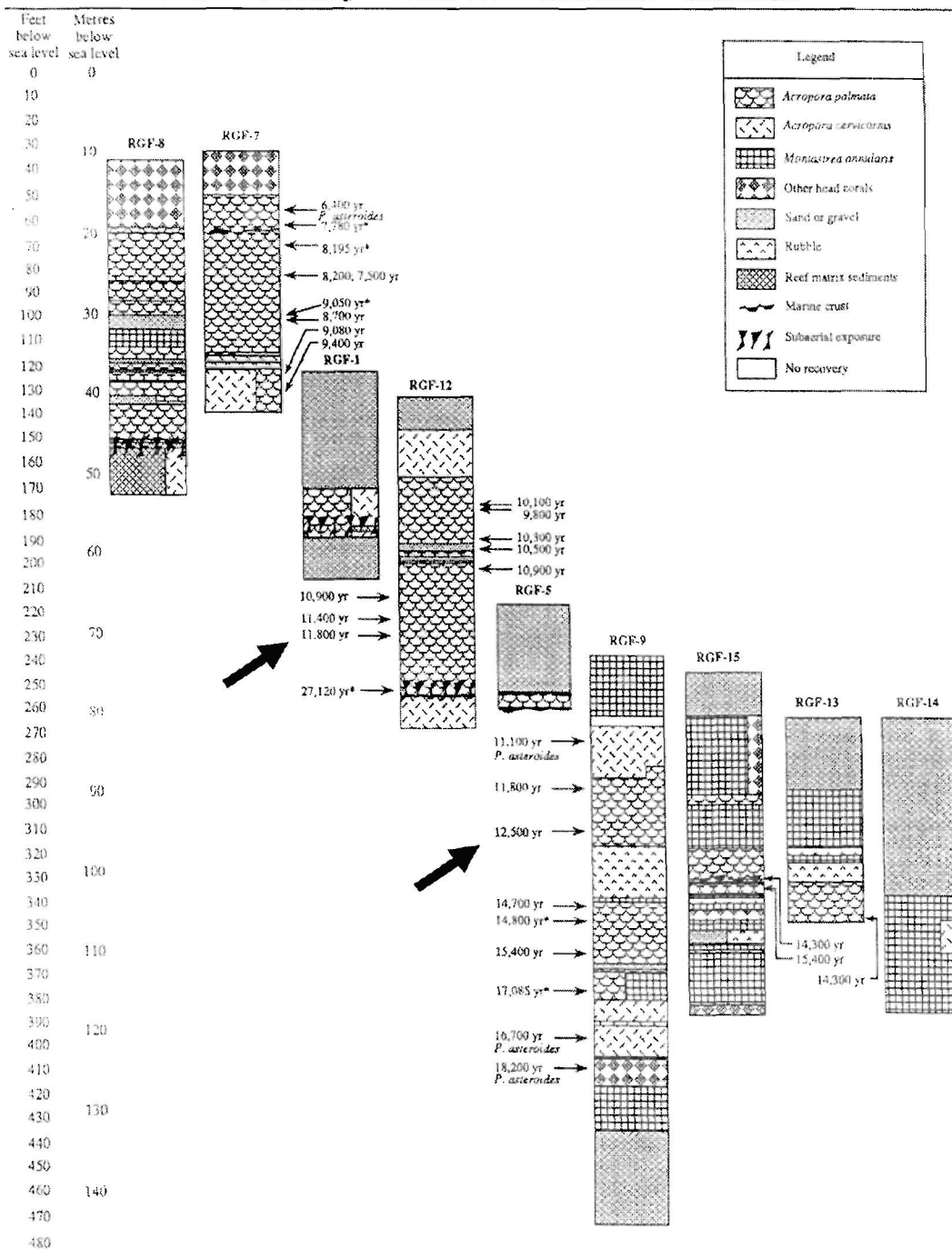


**Fig. 2.** Stratigraphic description for the nine longest cores recovered from Barbados. Large arrows indicate the two sample locations that were used to bracket the timing and magnitude of MWP 1A. Note that the sea-level jump is evident between 12,500 and 11,800  $^{14}\text{C}$  years B.P. only by comparing cores RGF-9 and RGF-1; not any one core contains direct evidence for a meltwater pulse. From Fairbanks (1989).

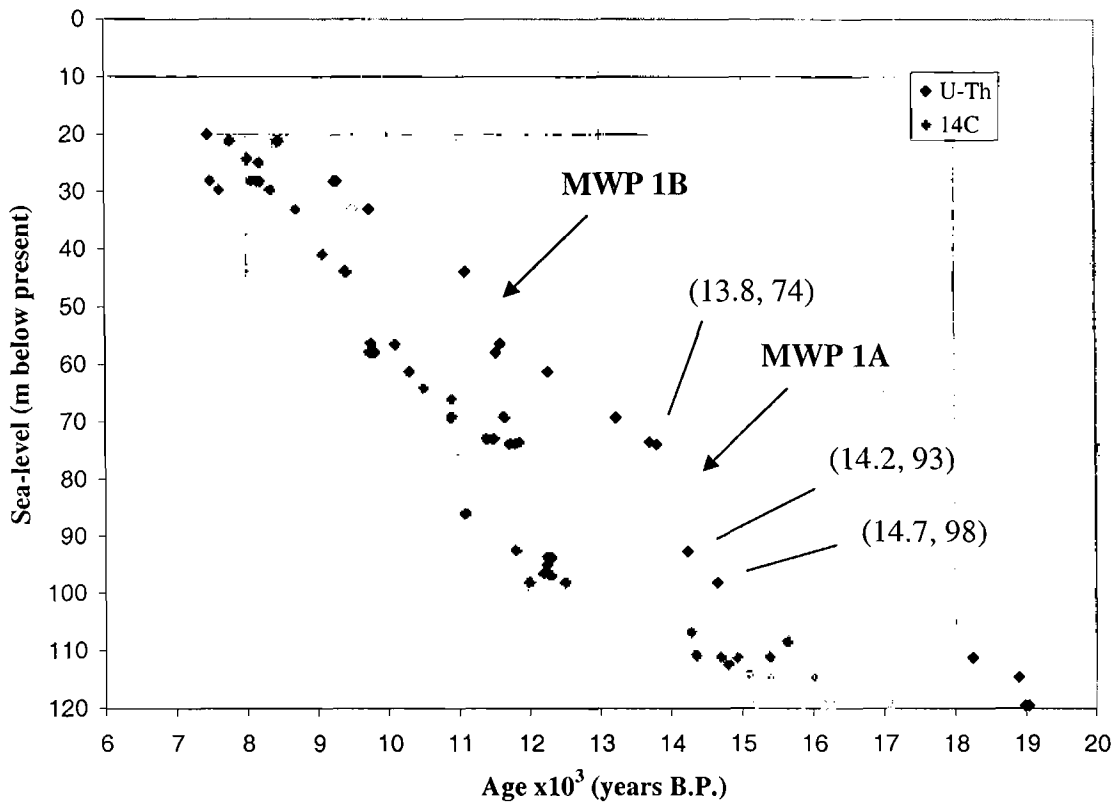


**Fig. 3.** Barbados sea-level reconstructions derived from <sup>14</sup>C (Fairbanks 1989) and U-Th data (Bard *et al.* 1990). The radiocarbon dates are not calibrated, but they show a 400-year marine reservoir correction. MWP 1A and B are arrowed. The most rapid rate of sea-level rise evident from these data occurred between 14,200 and 13,800 calendar years B.P.

years and 11,800 +/- 200 <sup>14</sup>C years B.P.). Furthermore, the apparent break in stratigraphy occurs between two cores, casting doubt on the validity of the inferred meltwater pulse.

## 2.2 Record from Tahiti

A signal of MWP 1A has been recognized in cores retrieved from coral terraces in Tahiti in the tropical Pacific (Fig. 4) (Bard *et al.* 1996). Unlike Barbados, this region is far from any plate boundaries and therefore is probably a relatively stable tectonic setting. In addition, Tahiti is far from locations of former ice sheets that could complicate the sea-level record with hydro-isostatic response.

Two cores were collected from the outer barrier reef flat that protects Papeete Harbor (Fig. 5). The compound vertical sequence of reef carbonates extends to a depth of 114 m and terminates at the basaltic substratum. An unconformity with evidence of subaerial exposure was identified at 86-87 m depth. Immediately above this hiatus, a single coral sample in a unit dominated by *A. robusta* and *Pocillopora verrucosa* was dated at about 13,750 +/- 30 calendar years B.P. (11,790 +/- 220 <sup>14</sup>C years B.P.). There are not any age data below the unconformity. Other cores drilled in the Tahiti barrier reef also preserve a hiatus and at least one *A. palmata* sample was dated at 13,850 calendar years B.P. The break in stratigraphy has been correlated to that observed at Barbados and may be the result of rapid sea-level rise during MWP 1A. However, these data are not direct evidence of a meltwater pulse. Thus, MWP 1A is again inferred from a sparse data set.

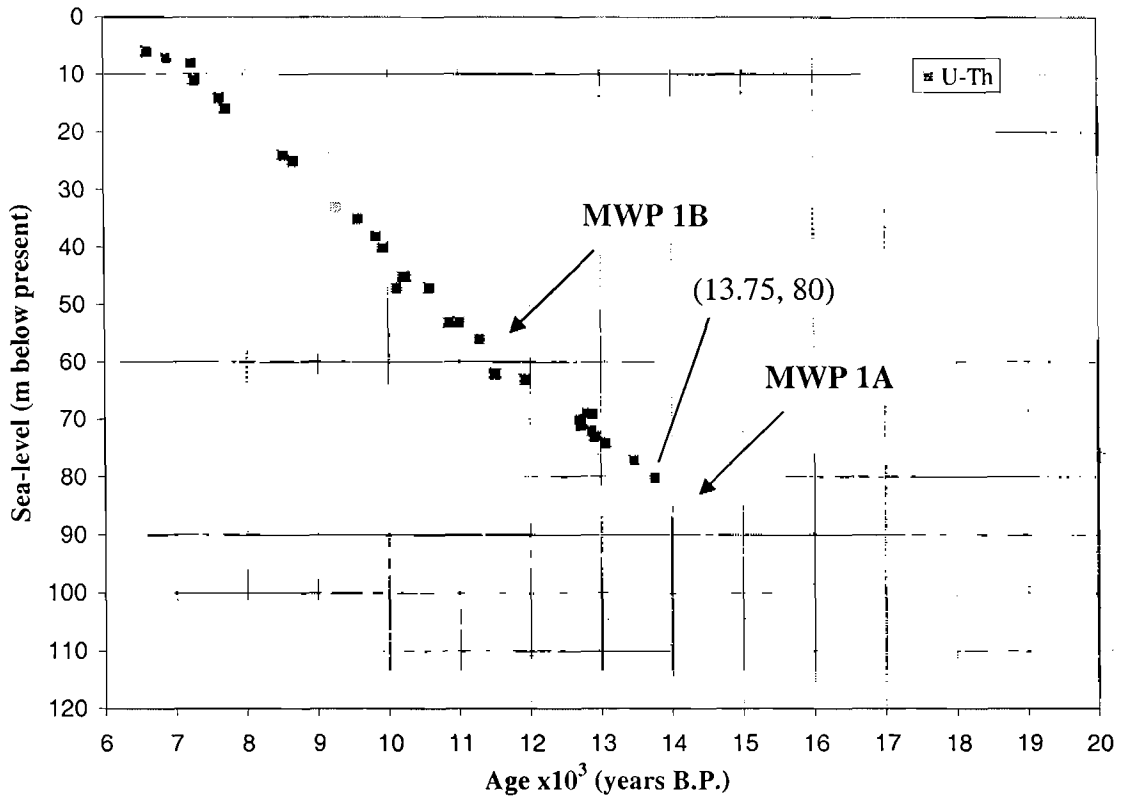


**Fig. 4.** The Tahiti sea-level reconstruction derived from U-Th (Bard *et al.* 1996) data. A hiatus that ended by 13,750 calendar years B.P. is thought to represent the end of MWP 1A. Note that these data afford a sea-level of 80 m below present immediately after the jump; however, the Barbados data (Fig. 3) indicate that sea-level stood at 74 m at 13,800 calendar years B.P.

## Barrier reef drillings (Tahiti, Papeete)

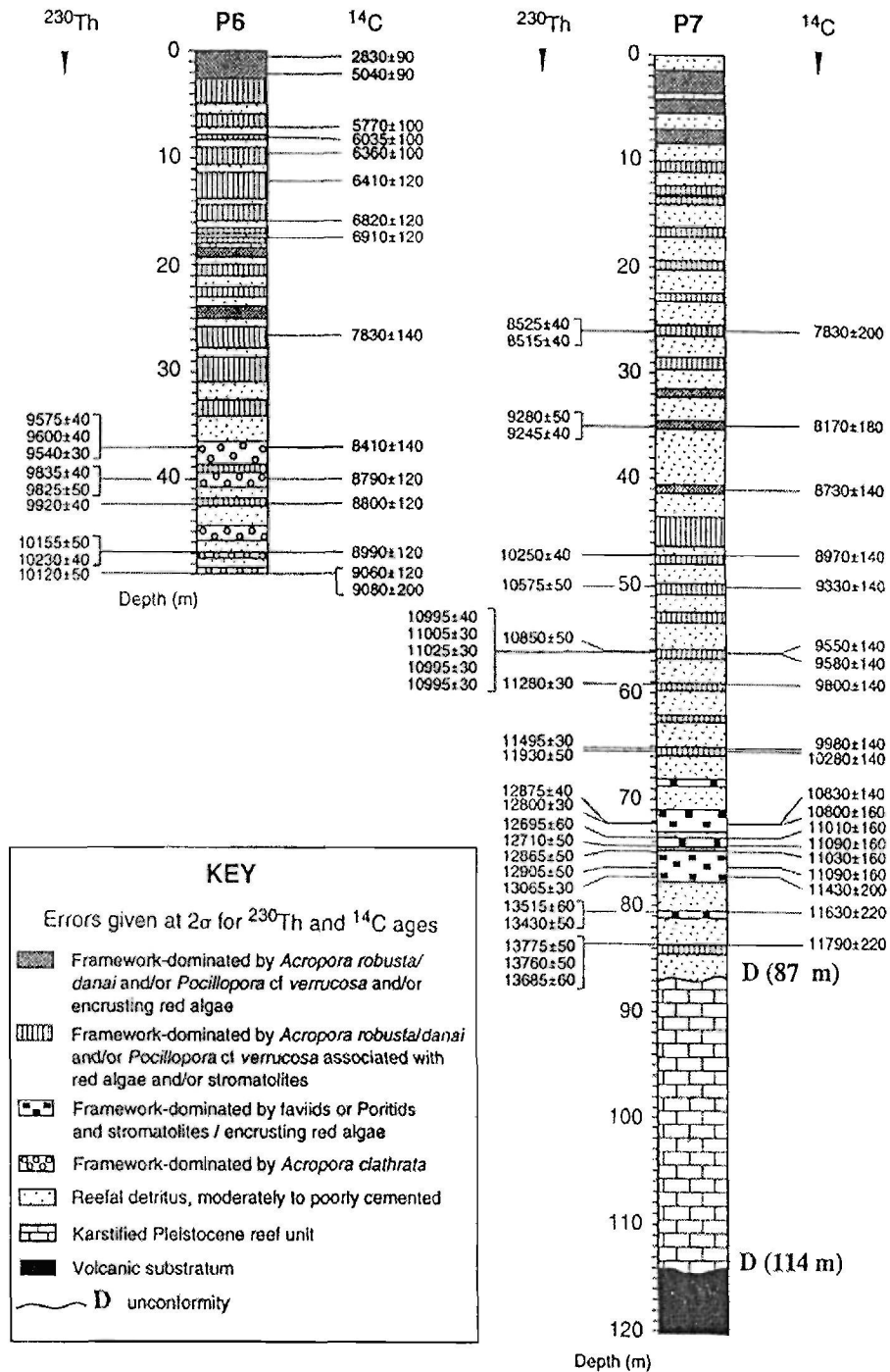


**Fig. 5.** Stratigraphic description for cores P6 and P7 from Tahiti. Note that the bottommost dated sample (~13,750  $^{14}\text{C}$  years B.P.) in core P7 is about 5 m above an undated unconformity. An abrupt rise in sea-level (MWP 1A) might explain the hiatus. From Bard *et al.* (1996).

### 2.3 Record from the Sunda Shelf

A third record of MWP 1A is that from the tectonically stable Sunda Shelf between the Indonesian archipelago and Vietnam (Hanebuth *et al.* 2000). In contrast to cores recovered from coral reef frameworks at Barbados and Tahiti (*e.g.*, Fairbanks 1989 and Bard *et al.* 1996), drill cores retrieved from the Sunda Shelf penetrated terrestrial organic material that grew near former sea level during a late-glacial transgression of the South China Sea. Atomic Mass Spectrometry (AMS) radiocarbon dates were obtained from identifiable samples that included mangrove roots, centimeter-size wood fragments, and coarse-grained peaty detritus in tidal-flat deposits. Tidal range on the shelf is 2 m, and therefore a higher precision sea-level reconstruction is possible than that based on corals (+/- 5 m precision).

The sea-level curve (Fig. 6) derived from shoreline facies extends from 21,000 to 13,000 calendar years B.P. (17,700-11,500  $^{14}\text{C}$  years B.P.). As with the Barbados data, the first stage of deglaciation following the LGM is gradual, with an average rate of sea-level rise of about 4 mm/yr. The onset of MWP 1A is thought to be marked by a cluster of data points at ~93 m core depth, with measured ages ranging from 15,300 to 14,400 calendar years B.P. (12,650 +/- 60-12,440 +/- 80  $^{14}\text{C}$  years B.P.). Two data points at 80 m core depth indicate that the event was over between 14,320 and 14,280 calendar years B.P. (12,360 +/- 70 and 12,290 +/- 70  $^{14}\text{C}$  years B.P.). Therefore, MWP 1A is postulated to have had a magnitude of 16 m and occurred between ~80 and 1020 calendar years. However, Hanebuth *et al.* (2000) favor a 16-m sea-level rise in 300 years which yields a ~53 mm/yr rate of change.

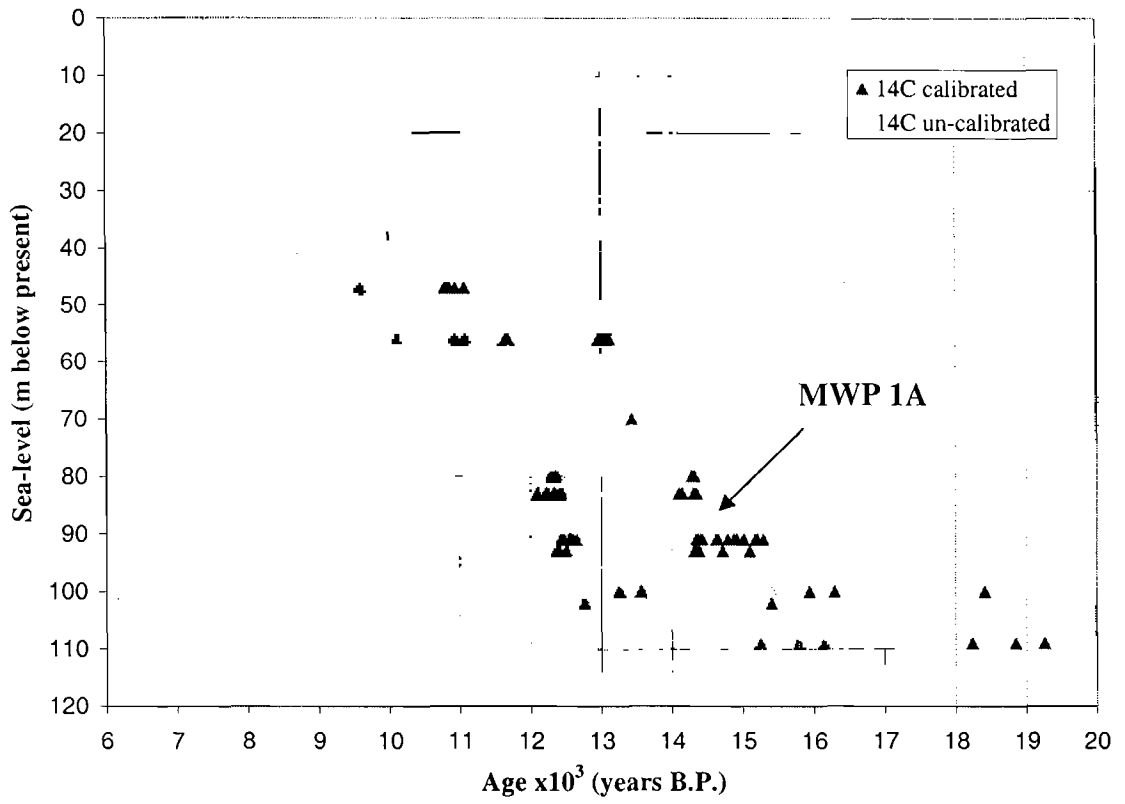


**Fig. 6.** The Sunda Shelf sea-level reconstruction (Hanebuth *et al.* 2000).



The Sunda Shelf sea level record is not without discrepancy. One severe problem is that numerous age reversals are observed in the stratigraphy (Fig. 7). Second, a clear MWP 1A signal is not registered in any one drill core, but instead inferred from a compilation of data from multiple cores. Thus, the sea-level jump is again poorly defined.

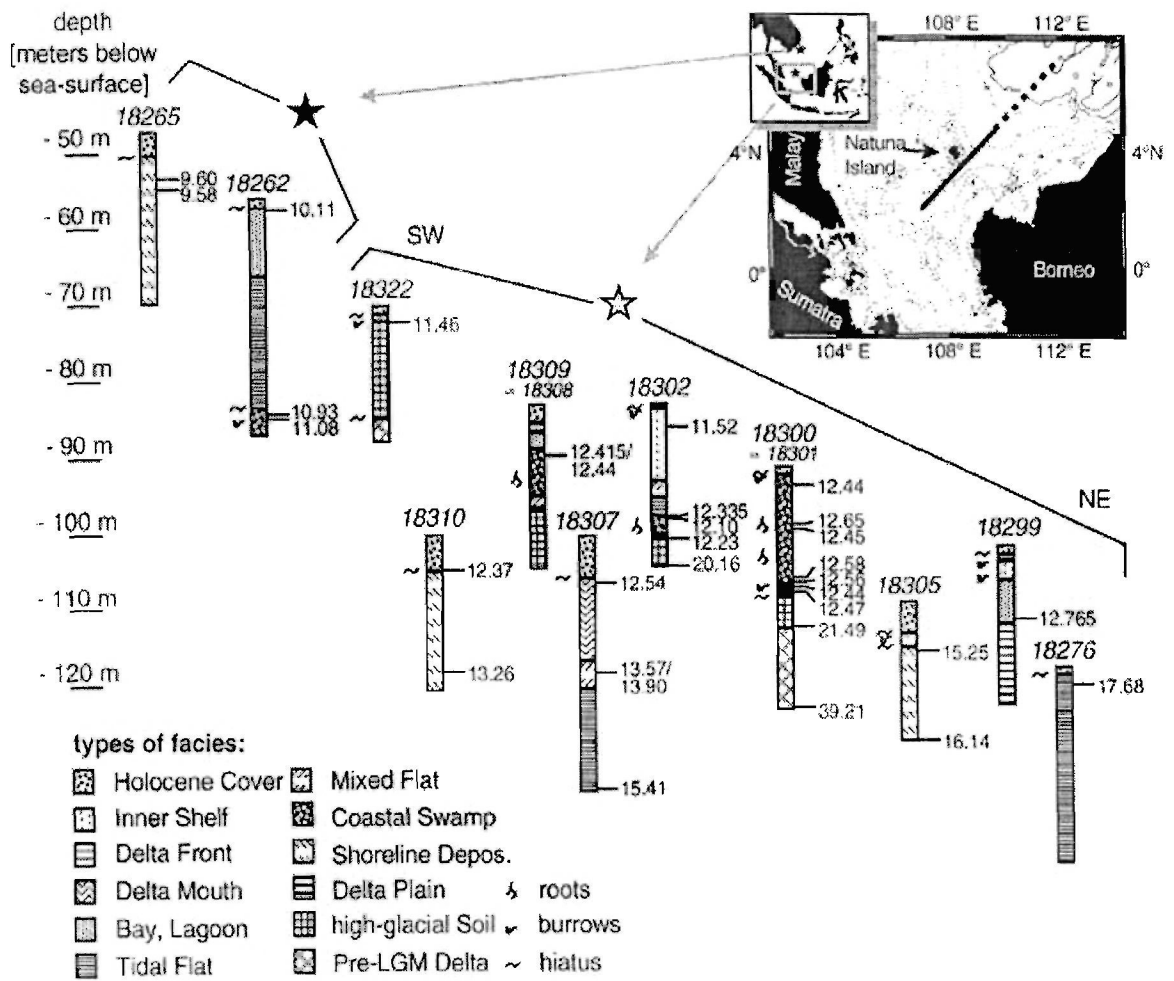
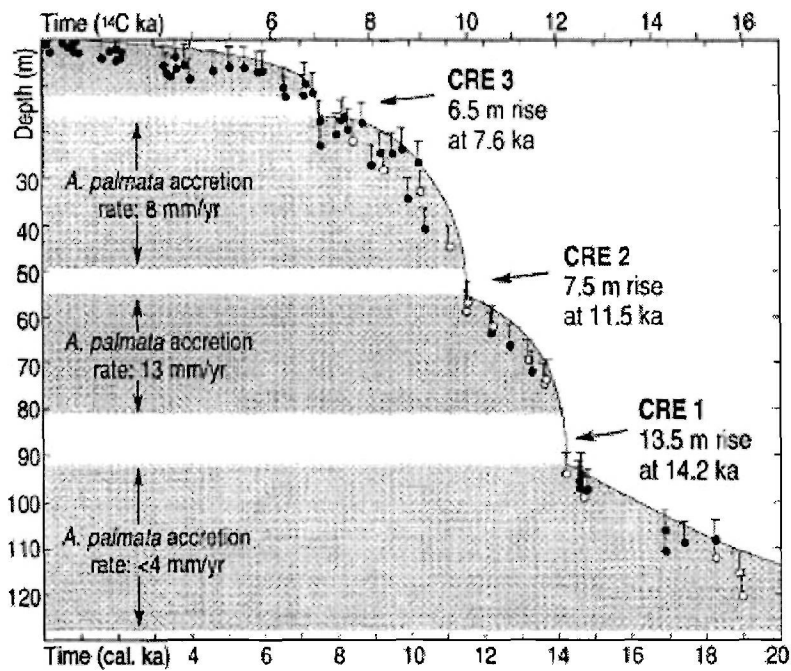


Fig. 7. Sunda Shelf stratigraphy. Note the age reversals in cores 18300 and 18302. From (Hanebuth *et al.* 2003 *Science* supplementary material).

## 2.4 Records from other Locations

At least two additional studies revealed evidence for MWP 1A. 1) Corals drilled on the Huon Peninsula in Papua New Guinea (Chappell and Polach 1991; Edwards *et al.* 1993) afford a sea-level reconstruction compatible with that from Barbados. The record, truncated by an unconformity, extends only to 13,129 calendar years B.P. (10,970  $^{14}\text{C}$  years B.P.). The hiatus is assumed to correlate to that observed at Barbados and Tahiti. 2) A Catastrophic Rise Event (CRE) (synonymous to MWP 1A) was identified in the Caribbean Atlantic based on measured displacements of *A. palmata* corals from monospecific to mixed reef frameworks (Blanchon and Shaw 1995). *A. palmata* reefs have a maximum accretion rate of 14 mm/yr (Buddemeier and Smith 1988) and the frameworks remain monospecific at water depths of less than 5 m. A rate of sea-level rise that exceeds 14 mm/yr will suppress *A. palmata* coral growth; however, the animals can develop in mixed reef frameworks in water depths to about 10 m (Goreau 1959). Applied to drowned *A. palmata* reefs in the Caribbean Atlantic, these constraints afford an abrupt 13.5 m rise in sea-level starting about 14,200 calendar years B.P. and ending in less than 290 calendar years.

The sea level curve produced by Blanchon and Shaw (1995) (Fig. 8) is a compilation of data from throughout the Caribbean Atlantic. Measurements from Barbados (Fairbanks 1989) were included in the composite record; however, a clear distinction was not made between those data collected by Blanchon and Shaw (1995) and those obtained by Fairbanks (1989). Therefore, it is difficult to cite Blanchon and Shaw (1995) as independent evidence of MWP 1A.



**Fig. 8.** Caribbean deglacial sea-level reconstruction. Drowned *A. palmata* reef frameworks are shown in light shading. Curve includes data from Barbados (Fairbanks 1989; Bard *et al.* 1990). U-Th data are shown with black dots; open circles represent calibrated radiocarbon sample ages. From Blanchon and Shaw (1995).

Figure 9 shows a compilation of sea level datasets. It is important to note that only records from Barbados (Fairbanks 1989; Bard *et al.* 1990) and the Sunda Shelf (Hanebuth 2003) show an abrupt meltwater pulse *ca.* 14,000 calendar years B.P. Data obtained from Tahiti (Bard *et al.* 1996) and Papua New Guinea (Chappell and Polach 1991; Edwards *et al.* 1993) only corroborate the existence of a hiatus after the postulated sea-level jump. Moreover, a MWP 1A signal is not recorded in any one core from Barbados; instead, it is inferred from a stratigraphic break between two cores. Sunda Shelf data would afford strong evidence of MWP 1A, but unfortunately the record is contaminated by numerous radiocarbon age reversals. Thus, the magnitude and timing of the meltwater pulse is not certain and the event itself is unproven. However, for the purpose of this study, I assumed that presumptions of MWP 1A are correct.

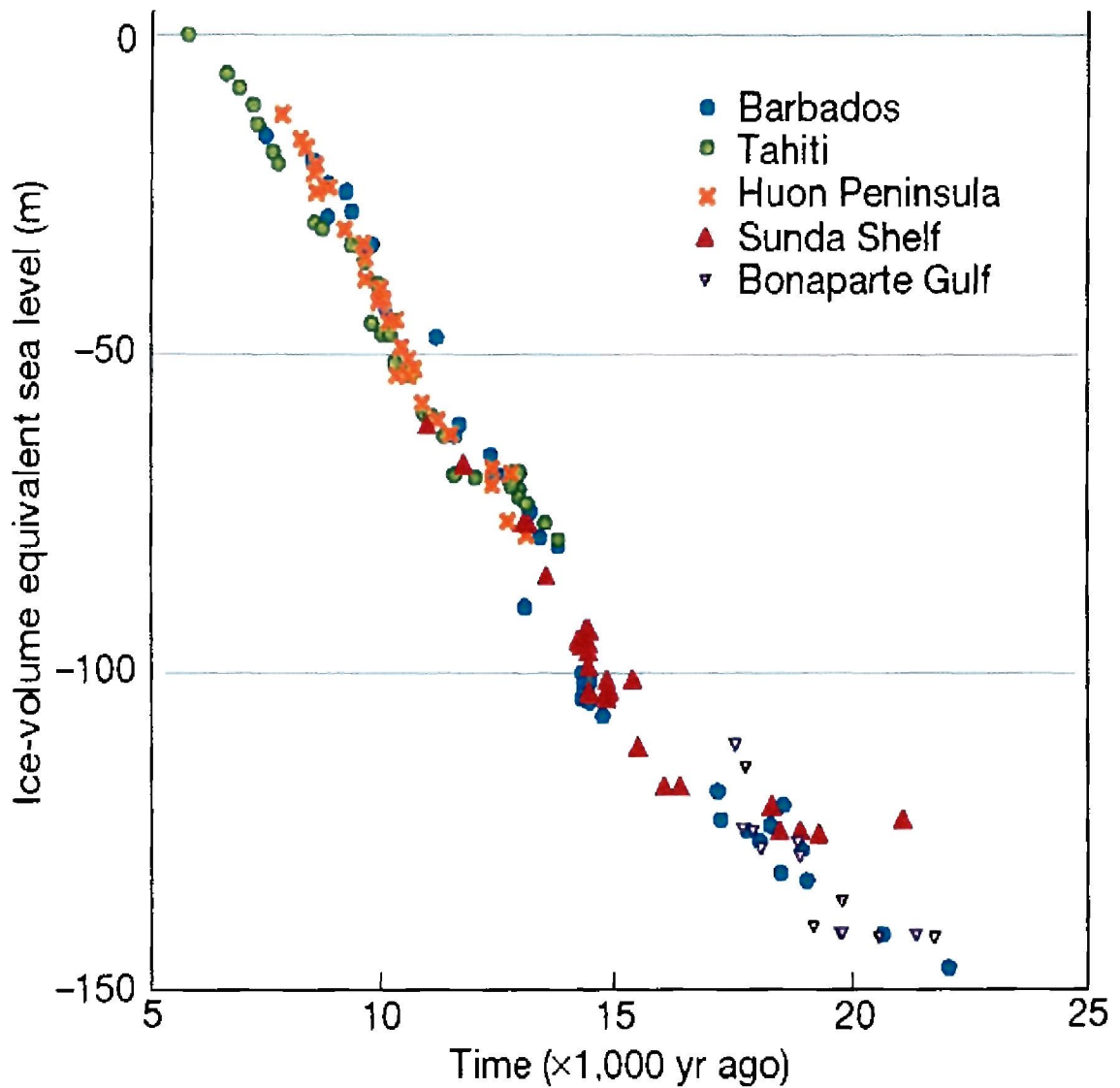


**Fig. 9.** Sea level data from Barbados (Fairbanks 1989), Tahiti (Bard *et al.* 1996), Huon Peninsula (Chappell and Polach 1991), Sunda Shelf (Hanebuth *et al.* 2000) and the Bonaparte Gulf (Yokoyama *et al.* 2000). Data from the Bonaparte Gulf precede MWP 1A and are therefore not discussed in the text. Modified from unknown source.

### 3. PREVIOUS INTERPRETATIONS OF MELTWATER PULSE 1A

#### 3.1 *Did MWP 1A originate in the Northern Hemisphere?*

Fairbanks (1989) assumed that MWP 1A originated in the Northern Hemisphere. This is a reasonable assessment because the Laurentide, containing ~80 m ice volume in sea-level equivalence (s.l. equiv.) at the LGM, was the largest of the former ice sheets. Moraine belts in the Great Lakes region show that the LIS extended as far south as 37° N latitude. This mid-latitude configuration indicates that at least a portion of the LIS was temperate and probably had significant seasonal surface ablation. Deep-sea cores collected in the North Atlantic show that ice streams in the Hudson Strait and Gulf of St. Lawrence regions episodically discharged armadas of icebergs into the North Atlantic during Heinrich events (Bond *et al.* 1992), however, none of which coincides with the timing of MWP 1A.

Changes in freshwater discharge to the world ocean affect global circulation. Modern marine precipitation and river discharge are redistributed by surface currents within the North Atlantic and result in strong vertical oxygen-isotope gradients. North Atlantic deep water (NADW) is produced by winter cooling, which causes downward convection of saline surface waters (Peixoto and Oort 1992). This process in turn is part of the global thermohaline conveyor that redistributes heat and salt throughout the world oceans. Low surface salinities can stabilize the vertical density profile, thereby inhibiting convection (Peixoto and Oort 1992). A sufficiently large discharge of freshwater, one the magnitude of MWP 1A, could conceivably disrupt the production of NADW, thereby

flipping the mode of thermohaline circulation. Total present-day discharge into the North Atlantic is 11,400 km<sup>3</sup>/yr (Baumgartner 1975). The discharge of MWP 1A may have been as high as 14,000 km<sup>3</sup>/yr (Fairbanks 1989). For comparison, the Mississippi and St. Lawrence Rivers discharge 560 km<sup>3</sup>/yr and 330 km<sup>3</sup>/yr respectively (Baumgartner 1975).

Deep sea records that contain microorganisms can be used to determine the past variability of discharge of the LIS. Isotopic composition of planktonic foraminifera is dependent upon temperature and the composition of ambient seawater. Cores retrieved from the North Atlantic (*e.g.*, Bard *et al.* 1987) show  $\delta^{18}\text{O}$  minima in the latter part of Termination Ia for *G. bulloides* at 13,600 and 12,300 <sup>14</sup>C years B.P., which correlates to MWP 1A and 1B. In addition, low  $\delta^{18}\text{O}$  values indicative of increased freshwater discharge *ca.* 14,000 calendar years B.P. are also observed in cores from the Gulf of Mexico (Leventer *et al.* 1982) and the Bermuda Rise (Keigwin *et al.* 1991).

Broecker *et al.* (1988, 1989) reported analyses from cores indicating that maximum discharge into the Gulf of Mexico occurred at ~12,000 <sup>14</sup>C years B.P., followed by minimum discharge from 11,100 to 10,500 <sup>14</sup>C years B.P. The elevated  $\delta^{18}\text{O}$  values were attributed to a diversion of glacial meltwater from the Mississippi to the St. Lawrence during the Younger Dryas. Such a scenario would lead to a decline of NADW formation and diminished northward advection of heat from subtropical surface waters. The net result could be a general cooling of the Northern Hemisphere. Similarly, Fairbanks (1989) suggested that a lowering of surface salinities over the North Atlantic could have triggered the Younger Dryas. However, a diversion of meltwater was unnecessary in this scenario. Instead, the observed sea-water freshening was the result of variable glacial meltwater production. In addition, Fairbanks (1989) also noted that the



effects of bioturbation had skewed the chronology of the cores used by Broecker (1988, 1989). The more precise chronology obtained at Barbados indicated that the slowdown preconditioned by NADW production probably began during the Bölling/Older Dryas time.

Bard *et al.* (1996) also speculated that the onset of the Younger Dryas could have been triggered by MWP 1A discharge into the North Atlantic. However, based on data from Tahiti, it was argued that the meltwater pulse occurred concurrently with the first major cooling of the Bölling-Alleröd between 13,900 and 13,800 calendar years B.P. This interpretation is incompatible with that suggested by Blanchon and Shaw (1995), whereby a so-called CRE occurred during the warmest segment of the Bölling-Alleröd ~14,200 calendar years B.P. (GRIP timescale). Hanebuth *et al.* (2000) offered another chronological assessment of MWP 1A, placing it between 14,700 and 13,800 calendar years B.P. This time frame is similar to that suggested by Blanchon and Shaw (1995) because it coincides with the warmest part of the Bölling-Alleröd (GISP2 timescale). However, the early-Bölling placement requires that MWP 1A had ended by the first major cooling of the period. This is inconsistent with the timing suggested by Bard *et al.* 1996.

Although interpretations regarding the timing and climatic importance differ, most previous workers (*e.g.*, Fairbanks 1989; Bard *et al.* 1990; Blanchon and Shaw 1995; Bard *et al.* 1996) attributed the source of MWP 1A to a partial collapse or rapid disintegration of some portion of the LIS. However, Clark *et al.* (1996) questioned this premise because offshore cores from the Hudson Strait (Andrews *et al.* 1994) and Gulf of St. Lawrence (Keigwin and Jones 1995) do not show lowered  $\delta^{18}\text{O}$  values during MWP

1A. Only cores recovered from the Gulf of Mexico (Leventer *et al.* 1982) and Bermuda Rise (Keigwin *et al.* 1991) indicate lowered  $\delta^{18}\text{O}$  values during MWP 1A consistent with an abrupt influx of meltwater. Because of this discrepancy, the southern margin of the LIS was cited as the only likely source for MWP 1A if the event occurred in the Northern Hemisphere (*e.g.*, Bard 1992).

Clark *et al.* (1996) reviewed the spectrum of possible discharges of MWP 1A. Neglecting 100 to 140-year certainty range on the reported U-Th ages, the Barbados sea-level data afford a meltwater pulse of 19 m s.l. equiv. in 430 years (Bard *et al.* 1990) or a total discharge of  $\sim 0.43$  Sv (1 Sv =  $10^6$  m<sup>3</sup>/s). Similarly, Blanchon and Shaw (1995) reported that MWP 1A caused sea-level to rise 13.5 m in less than  $\sim 300$  years with a total discharge of  $\sim 0.52$  Sv. The average of these two discharges is  $\sim 0.5$  Sv. Clark *et al.* (1996) estimated that between 13,000 and 11,000 <sup>14</sup>C years B.P., meltwater was discharged through the Mississippi at  $\sim 0.03$  Sv accompanied by an equivalent rise in global sea-level of  $\sim 2.9$  m. In order to attain a discharge of 0.5 Sv into the Gulf of Mexico, the southern Laurentide would have to deflate vertically by at least 8 m/year. It seems unlikely that the southern Laurentide could have ablated so rapidly. Therefore, a substantial meltwater contribution could have come from elsewhere. Clark *et al.* (1996) noted that the only other plausible source for MWP 1A was the Antarctic Ice Sheet (AIS).

### 3.2 Did MWP 1A originate in the Southern Hemisphere?

A geophysical model was developed to “fingerprint” the source of MWP 1A based on the principle that any large ice mass will gravitationally attract ocean water

(Clark *et al.* 2002). By considering the amount of ice volume lost and subsequent isostatic rebound in North America, Antarctica and the Barents Sea, a gravitational departure from mean global sea level could be calculated for any region on the globe. For a meltwater pulse originating from the southern sector of the Laurentide Ice Sheet, a 25-m sea-level rise should have occurred at Barbados, whereas sea-level rise at the Sunda Shelf should have been 38 m. This difference is not observed in the sea-level curves reconstructed by Fairbanks (1989) and Hanebuth *et al.* (2000). Instead, sea level at each site where MWP 1A has been identified appears to have been roughly equivalent. This observation fits model scenarios only in which much or all meltwater for the sea-level jump came from Antarctica.

With these results supporting an Antarctic-sourced meltwater pulse, Weaver *et al.* (2003) used an intermediate-complexity climate model to simulate an abrupt influx of freshwater into the Southern Ocean to determine any effect it could have on thermohaline circulation. A pulse from the Antarctic Peninsula into the region of Antarctic intermediate water (AAIW) production reportedly could perturb the global thermohaline conveyor and trigger deep water formation in the North Atlantic. In turn, this could serve as the mechanism that initiated the Bölling-Alleröd warm period in the Northern Hemisphere.

There are severe problems with regard to the feasibility of a meltwater pulse originating from Antarctica. The AIS is polar and does not have a surface melting zone. Therefore, the hypothesis that MWP 1A originated from Antarctica requires a mechanical collapse driven by internal ice dynamics, rather than melting of surface ice. Furthermore, moraine mapping on the inland side of the Transantarctic Mountains indicates that

interior ice-surface elevations of the East Antarctic Ice Sheet (EAIS) have changed little since the LGM (Bockheim *et al.* 1989; Denton *et al.* 1989a, b). The most significant modification to that ice sheet occurred along the periphery where ice extended beyond the present-day position to the outer continental shelf at the LGM (Goodwin 1993; Miura *et al.* 1998).

Antarctica contained at most an additional 18 m (Huybrechts 2002), but probably less than 14 m (Denton and Hughes 2002) ice-volume s.l. equiv. at the LGM. Of the total volume lost since the onset of deglaciation, West Antarctica contributed two-thirds (Denton and Hughes 2002; Huybrechts 2002), with the remainder having come from East Antarctica. Therefore, West Antarctica is the most likely Southern Hemisphere ice-source for a meltwater pulse requiring a mechanical collapse.

One plausible mechanism by which enough ice-volume could be evacuated from the West Antarctic Ice Sheet (WAIS) to produce an event of the magnitude of MWP 1A is that of exploding ice shelves (Scambos *et al.* 2000). Meltwater produced during particularly warm summers could infiltrate crevasses and facilitate calving of large ice-slabs. Rapid shelf disintegration would reduce the back-stress at the grounding-line and ice streams would accelerate, thereby quickly draining interior ice.

A caveat to producing a meltwater pulse from exploding ice shelves in West Antarctica is that the deglacial chronology for the Ross Sea sector indicates a mid to late-Holocene recession, which is incompatible with the *ca.* 12,000 <sup>14</sup>C years B.P. or 14,000 calendar years B.P. timing associated with MWP 1A. Grounded ice extended to the continental shelf during the LGM on average 1000 km farther north than the present position (Licht *et al.* 1996; Shipp *et al.* 1999; Hall and Denton 2000). The grounding-line

retreated southward from the vicinity of Ross Island in McMurdo Sound between 6500 and 8340  $^{14}\text{C}$  years B.P. (Fig. 10) (Conway *et al.* 1999; Hall and Denton 2000). Grounded ice in the Weddell Sea might have also extended farther north towards the continental shelf than it does at present (Anderson and Andrews 1999) and probably has a similar retreat history to that of the ice sheet in the Ross Sea.

A mid to late-Holocene deglaciation of the Ross Sea Embayment coupled with a total ice-volume loss of only 14 m (s.l. equiv.) since the LGM seems to preclude the likelihood that MWP 1A could have come from Antarctica. However, the deglacial history of the East Antarctic Ice Sheet is not well known; therefore, it is possible that previous estimates of LGM ice-volume are low. Similarly, the disparity between predicted discharge from the southern Laurentide and comparatively high  $\delta^{18}\text{O}$  values observed in cores from the Gulf of Mexico and the Bermuda Rise during the time of MWP 1A weakens the case for a Northern Hemisphere meltwater source. Pinpointing the origin of MWP 1A, assuming it was real, requires both glacial geologic evidence and more detailed records of sea-level change. Until new information becomes available, models can be used to test the physical plausibility of existing hypotheses.

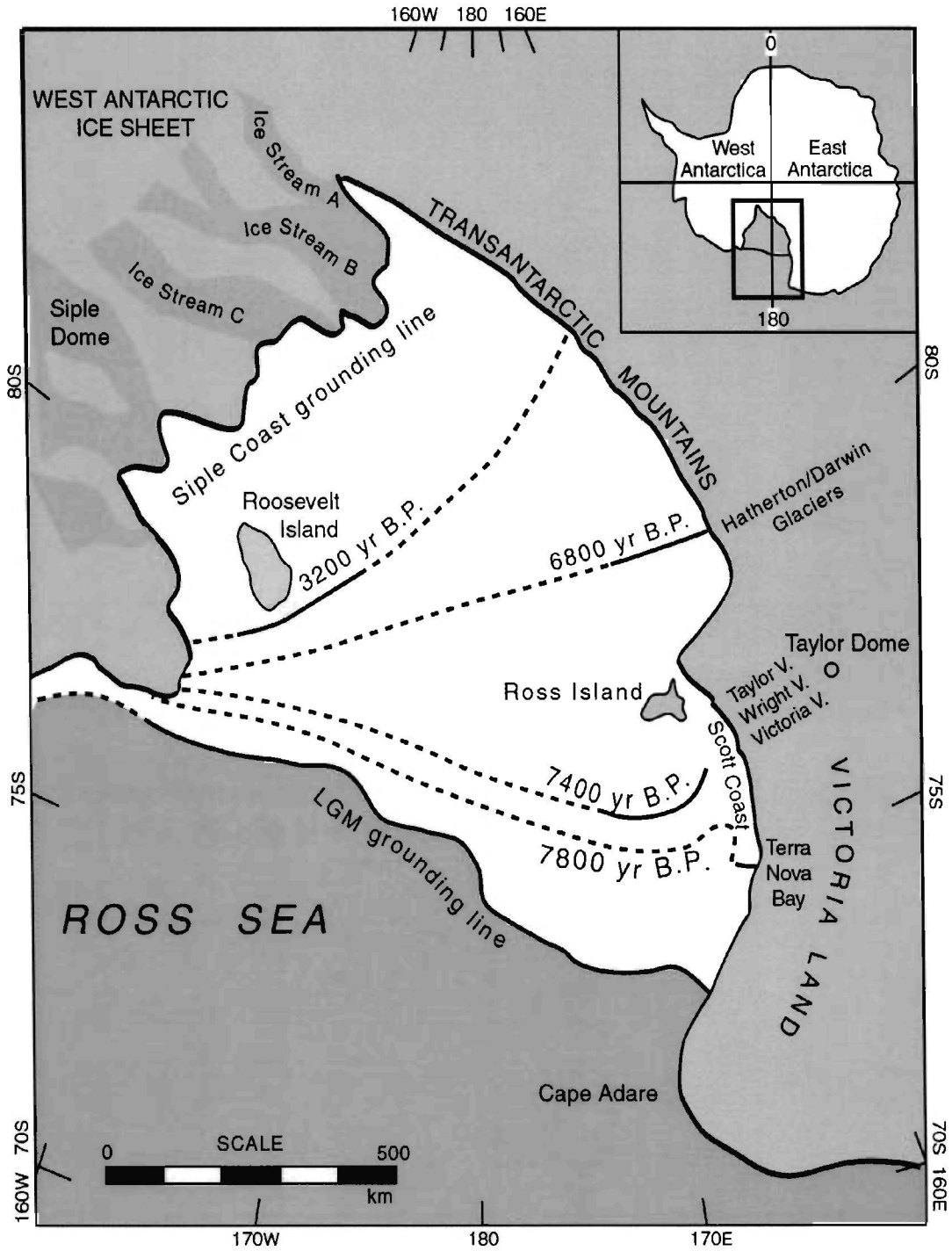


**Fig. 10.** Deglacial chronology of grounded ice in the Ross Sea region (modified from Conway *et al.* 1999).

## 4. METHODS

Previous geophysical studies (*e.g.*, Peltier 1994; Clark *et al.* 2002 and Weaver *et al.* 2003) evaluated either thermohaline perturbations or isostatic response of the crust to a meltwater pulse. Here, I take a glaciological approach by using the University of Maine Ice Sheet Model (UMISM) to test the hypothesis that the LIS was capable of producing a meltwater release consistent in magnitude and timing to that of MWP 1A.

The UMISM is a glaciological map-plane model that can derive both steady-state and time-dependent solutions (*see Appendix 1*). Time-dependent ice sheets are built from the ground up by using an embedded simple climatology module that can calculate accumulation and ablation (and therefore net mass-balance) at each node in the map plane based on mean-annual paleo-temperature input (*see Appendix 2*). For this study, I chose to use temperature data derived from ice-core records.

Input and initial conditions can greatly affect the end product of any computational model. Because ice-core data are used to establish climate in the UMISM, it is important to recognize chronology limitations. A timeseries can be derived from annual melt-layer counting (*e.g.*, GISP2), glaciological flow modeling (*e.g.*, GRIP, Vostok, EPICA Dome C) or by defining tie points whereby observed isotopic or chemical spikes correlate with dated events known from other paleo-climatic records. A given event can be assigned different ages in different cores; therefore model results do not follow an absolute age clock (Fig. 11).

Because of the inherent error associated with establishing chronology, events observed in ice cores are commonly reported in ice-core years. Accordingly, results from

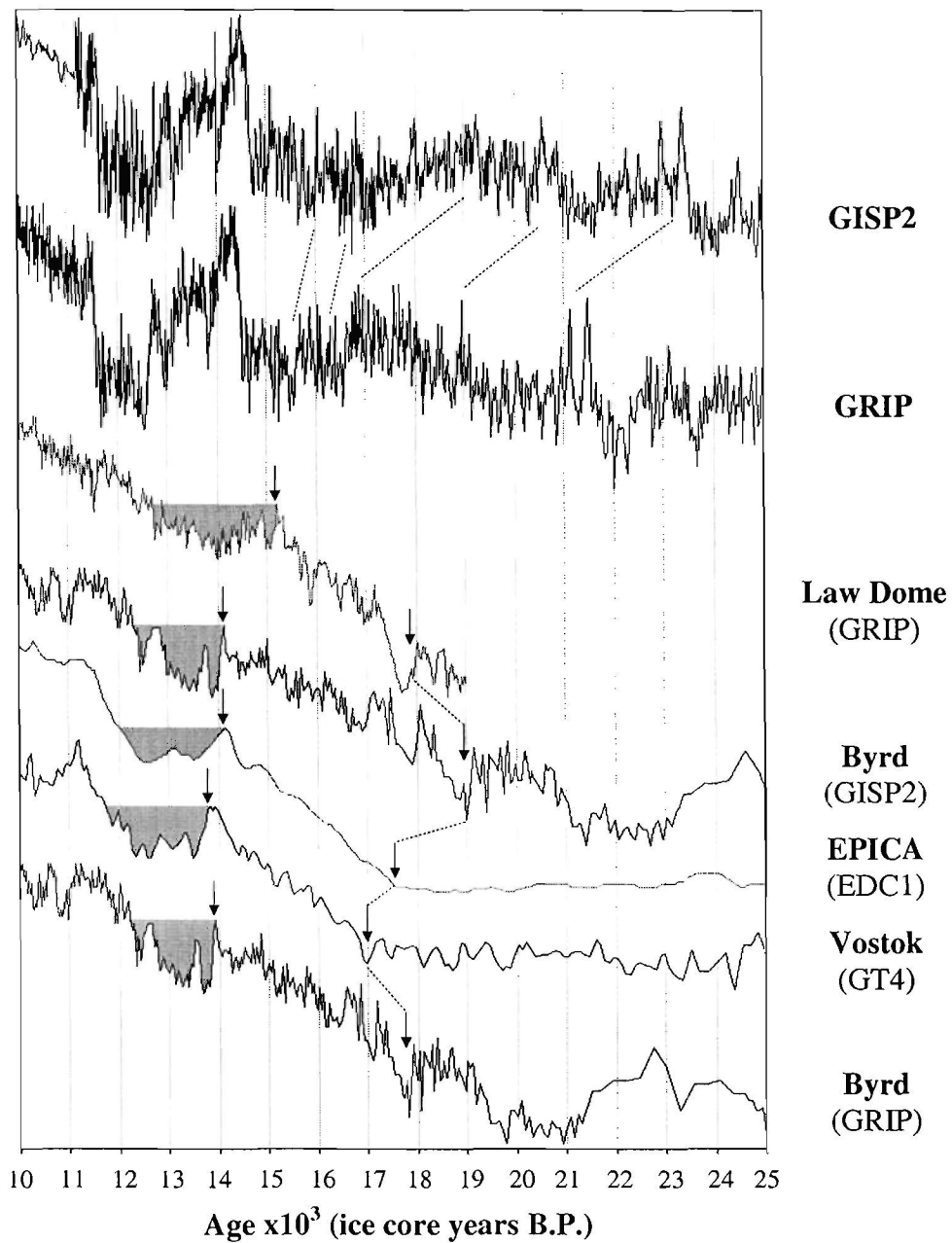


**Fig. 11.** Northern and Southern Hemisphere ice-core chronologies. The GISP2 chronology is based on annual melt-layer counting. The GRIP timescale is derived from annual melt-layer counting to 17,000 ice core years and glaciological flow modeling for the remainder of the record. The Law Dome chronology is tied to GRIP by a Younger Dryas methane spike (Morgan *et al.* 2002). Similarly, the two Byrd timescales are matched by methane to either GRIP (Blunier *et al.* 1998) or GISP2 (Blunier and Brook 2001). A <sup>10</sup>Be peak at 40,000 ice core years, volcanic events of known age and a methane rise at the end of the Younger Dryas serve as tie points between EPICA EDC-1 and the GRIP timeseries. These tie points were used by a glaciological flow model to derive the EDC-1 chronology (Schwander *et al.* 2001). The Vostok GT4 timescale was developed by Petit *et al.* (1999). Lines and arrows illustrate chronology differences. The Antarctic Cold Reversal (ACR) is shaded grey.



the UMISM are reported in model years, both to reflect the chronological error of the input data and to recognize error that may be inherent to the model itself. Caution must be used when model results are compared to events dated in  $^{14}\text{C}$  or  $^{234}\text{U}$ - $^{230}\text{Th}$  (calendar) years.

A number of simulations were conducted in an evolving fashion using the UMISM. Results from the first model run influenced the structure of the second and so forth; however, each simulation used certain default parameters in order to ensure consistency (*see Appendix I*). I have grouped the simulations into two experiments. In Experiment 1, the LIS was reconstructed by using the GISP2 ice-core record to drive the model. GISP2 was chosen because it affords a high resolution proxy of Northern Hemisphere climatic change. Furthermore, elevated temperatures are recorded in GISP2 during the onset of the Bölling-Alleröd (Fig. 12). I sought to test whether these changes were significant to generate a meltwater pulse. In contrast to the first experiment, Experiment 2 was conducted using the EPICA Dome C ice-core record as model input. This Antarctic record of climatic change has a different chronology and more subdued muted temperature oscillations compared to that of GISP2. It defies convention to model a Northern Hemisphere ice sheet using a Southern Hemisphere climate signal. Nevertheless, results from the EPICA experiment illuminated problems using GISP2.

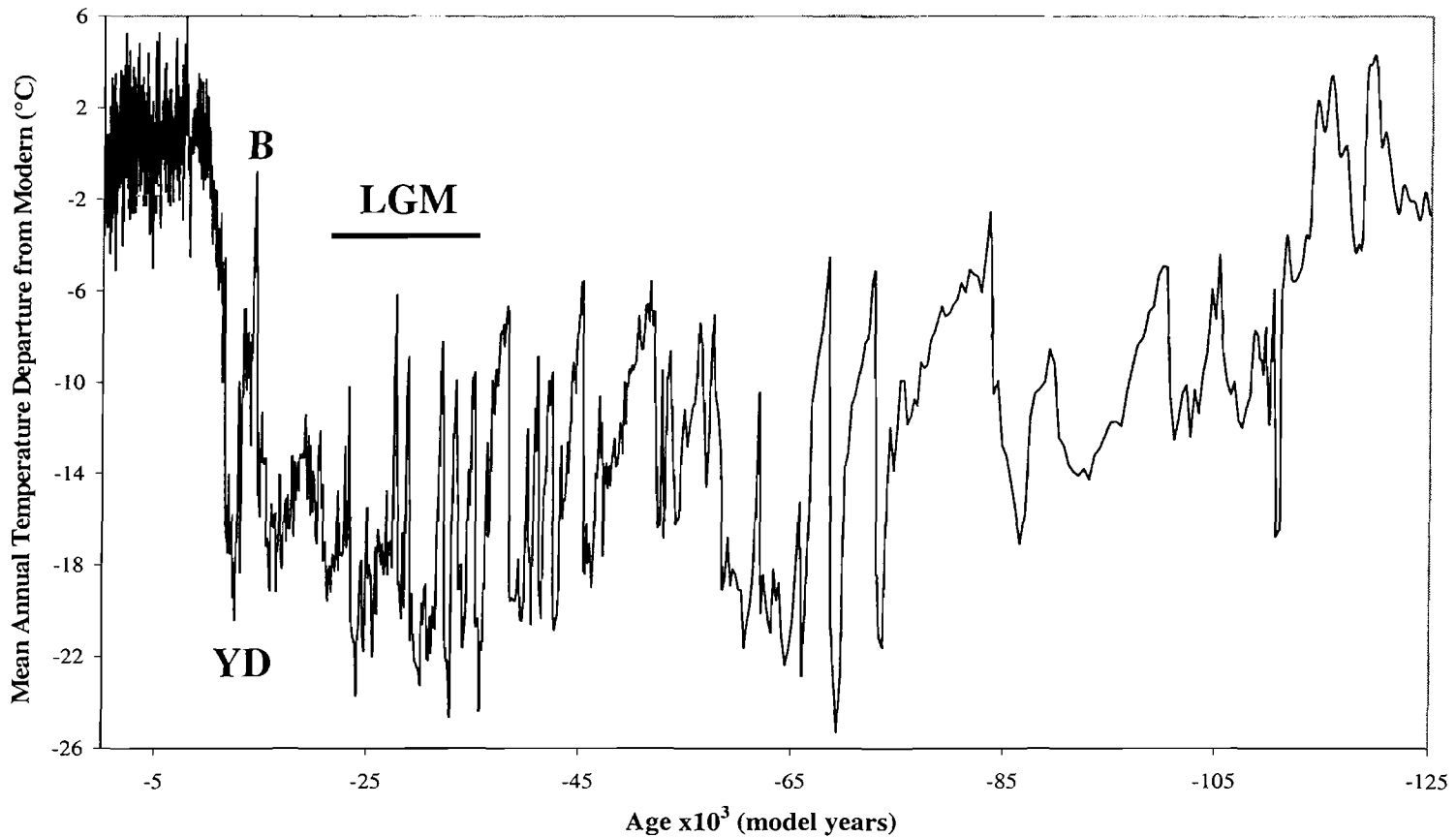


**Fig. 12.** The GISP2 record formatted for the UMISM. Mean annual temperatures are derived from oxygen isotope data (Cuffey and Clow 1997). Note that the LGM has a maximum temperature depression of about 23 °C. Warming during the Bölling (B) peak reaches to within about 1 °C from the modern temperature. The Younger Dryas (YD) here is characterized by as much as a 20 °C temperature depression. The original chronology developed for GISP2 extends only to 105,000 ice core years B.P. Data from the GRIP ice-core (Johnsen *et al.* 1997; and others) was spliced onto the record to extend the climate history to 125,000 ice core years B.P. for modeling purposes.

## 5. RESULTS

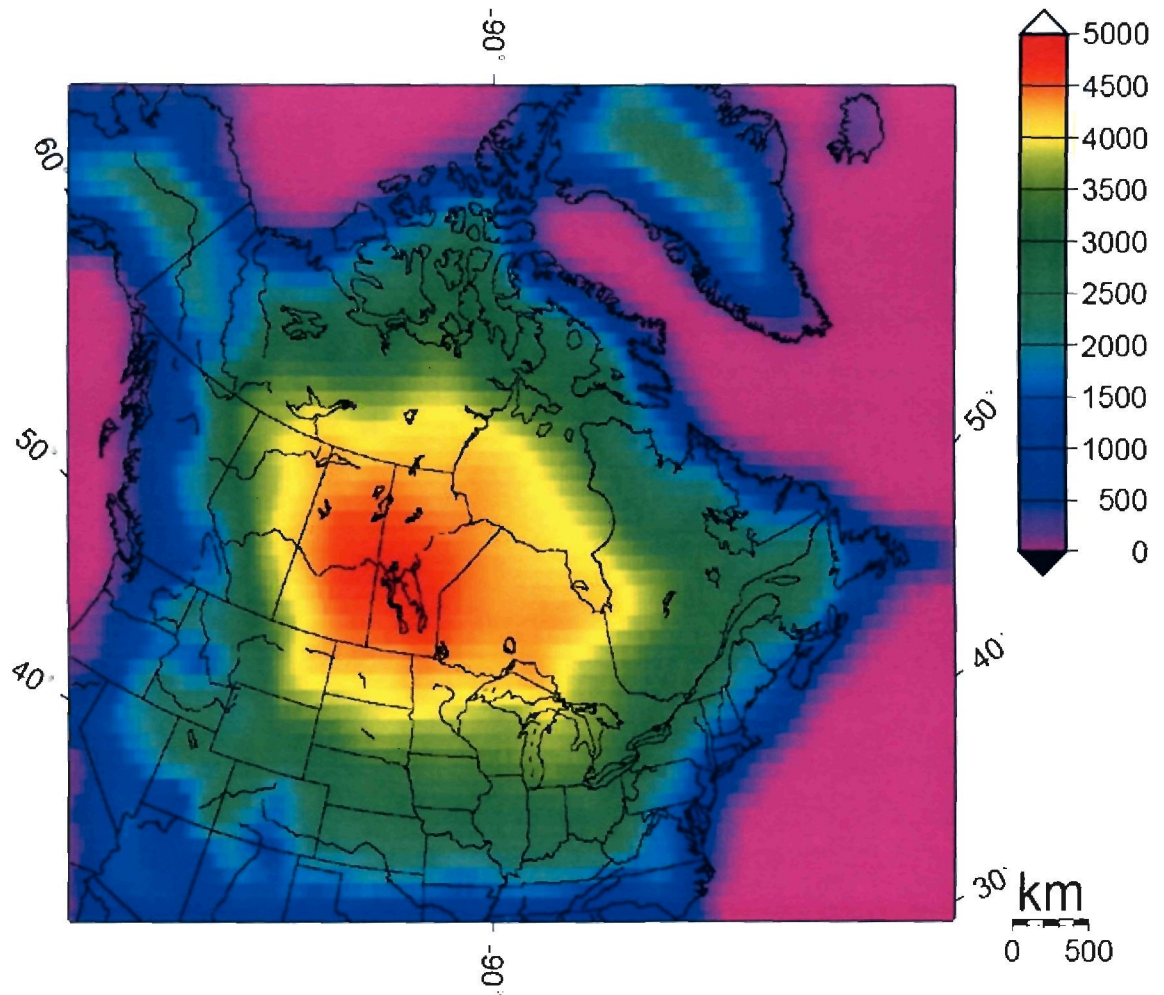
### *5.1 Experiment 1*

The UMISM was configured to run through a complete glacial cycle; however, the first simulation was ended at the LGM because an unrealistic ice sheet grew to engulf the entire North American continent (Fig. 13). This erroneous product resulted from the response of the model to a 23 °C mean-annual LGM temperature depression as recorded by GISP2.

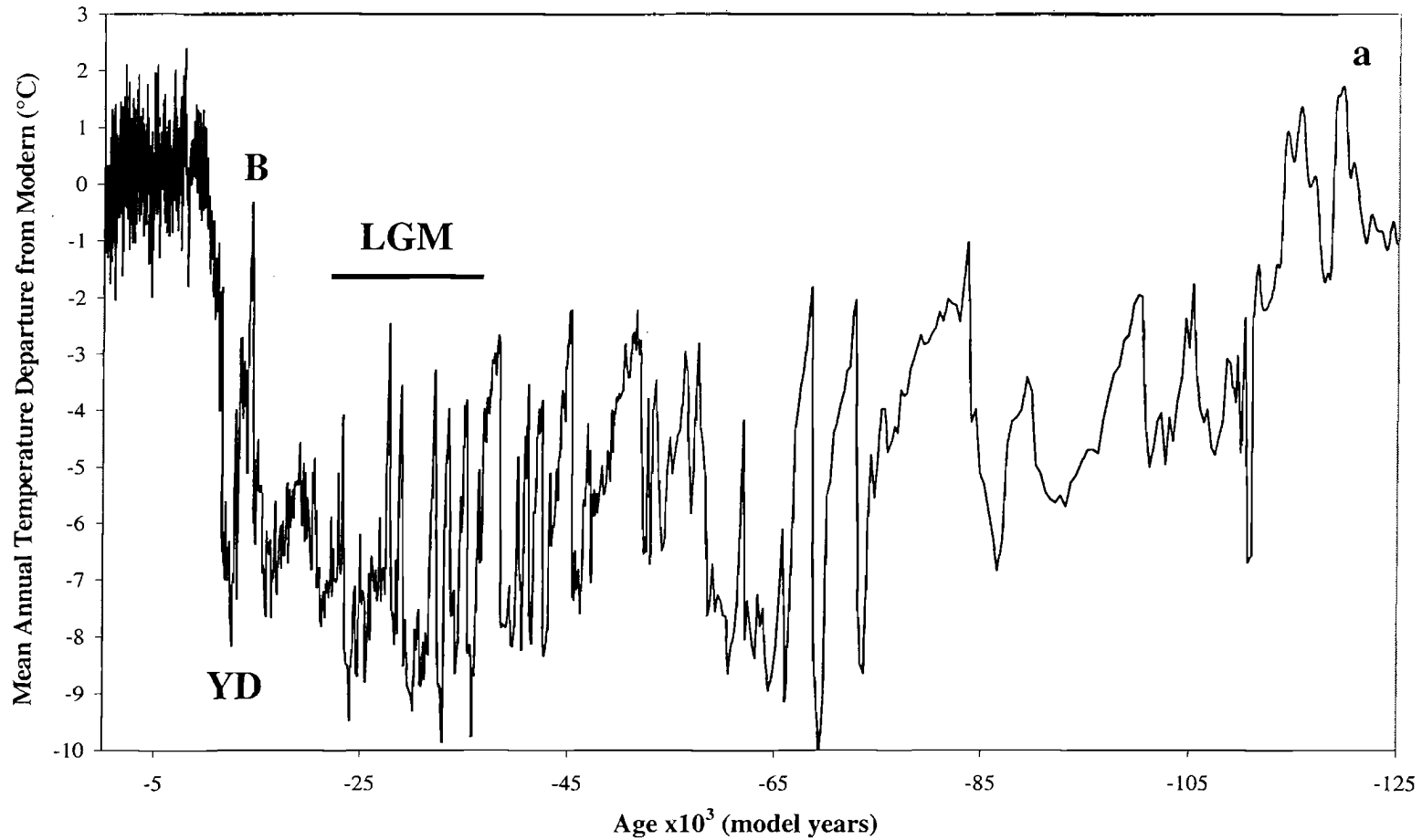
Because the glaciological response of a large ice sheet to climate will differ from that of a small ice sheet, it was critical to attain a realistic LGM baseline before testing for MWP 1A. In that vein, the over-voluminous LGM ice sheet generated in the first simulation could not be used for modeling MWP 1A. An ice sheet in better accord with existing geologic data was reconstructed in subsequent simulations by scaling the temperature input by 40% and 50% (Fig. 14a, b). Without any physical basis, I scaled GISP2 arbitrarily to make it work. The UMISM consistently produced a reasonable LIS with an LGM mean-annual temperature depression between 8.5 and 10 °C.

Two experiments were conducted using the scaled input (15a, b, c). For clarity and because results are nearly identical, here I describe only the second simulation, wherein the mean-annual temperature signal amplitude was reduced by 50%.

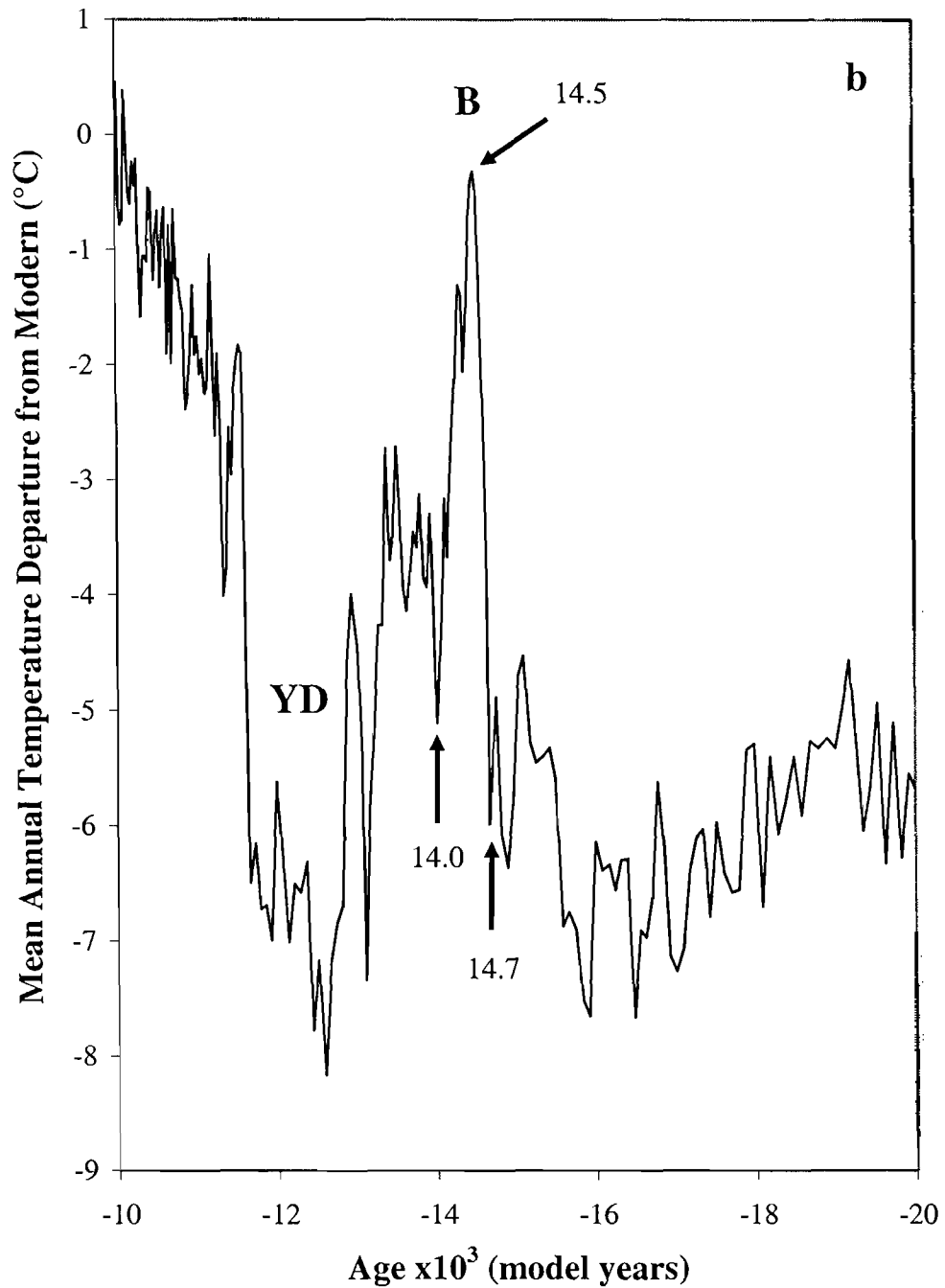
The pattern of glaciation for the first 100,000 years is broadly consistent with that known from sea-level reconstructions and other paleo-climate indicators (Fig. 16). However, the LGM is not well defined. Maximum ice buildup begins about -25,000



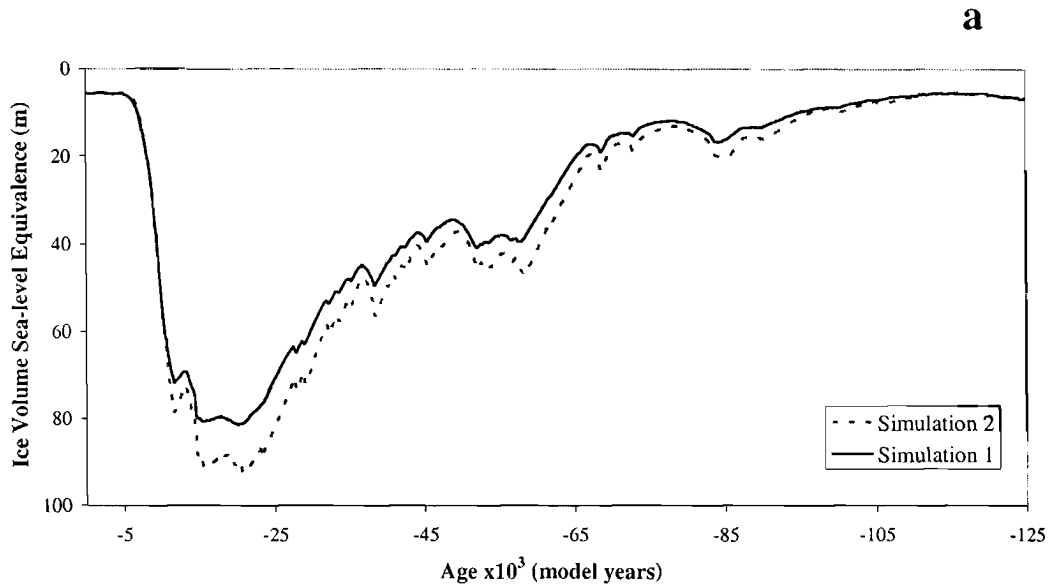
**Fig. 13.** Ice sheet generated by using the GISP2 record as a proxy for mean-annual temperature change. These results reflect a  $\sim 23^{\circ}\text{C}$  LGM temperature depression. Colors indicate ice thickness.



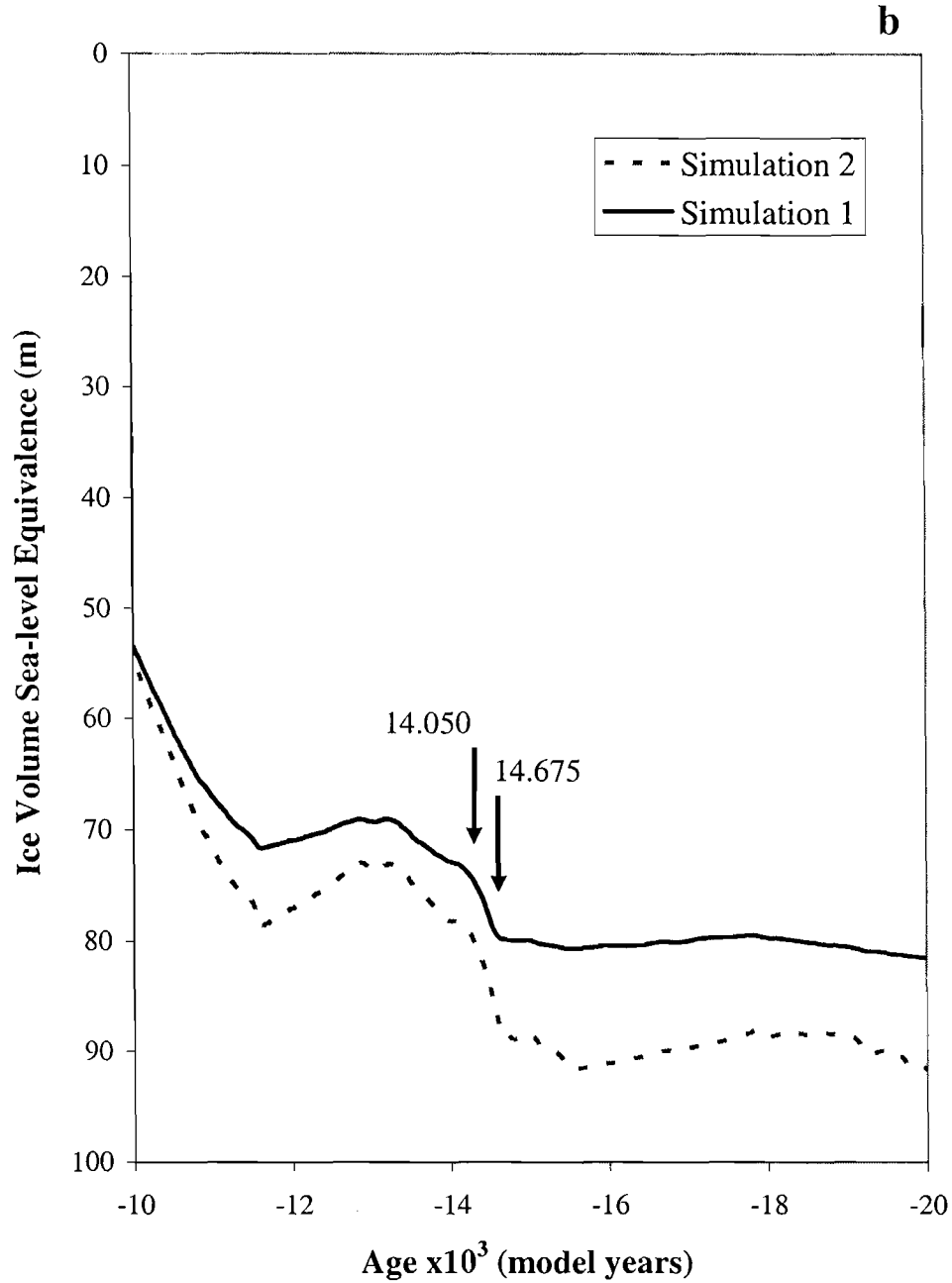
**Fig. 14.** The GISP2 temperature record. **a.** Formatted for the UMISM with the signal amplitude scaled 40%. Note that the LGM has a maximum mean-annual temperature depression between 8.5 and 10 °C. Warming during the Bölling (B) peak reaches to within about 0.5 °C from the modern temperature. The Younger Dryas (YD) here is characterized by 7 to 8 °C mean-annual temperature depression from the modern climate.



**Fig. 14.** Continued. **b.** The scaled GISP2 record showing from 20,000 to 10,000 ice core years B.P. 14,700 ice core years B.P. marked the start of the Bölling (B) warm spike. Peak warmth was reached by 14,500 ice core years B.P. and a sharp cooling at 14,000 ice core years B.P. marked the beginning of the Alleröd. The Younger Dryas (YD) has a maximum temperature depression of about 8 °C.

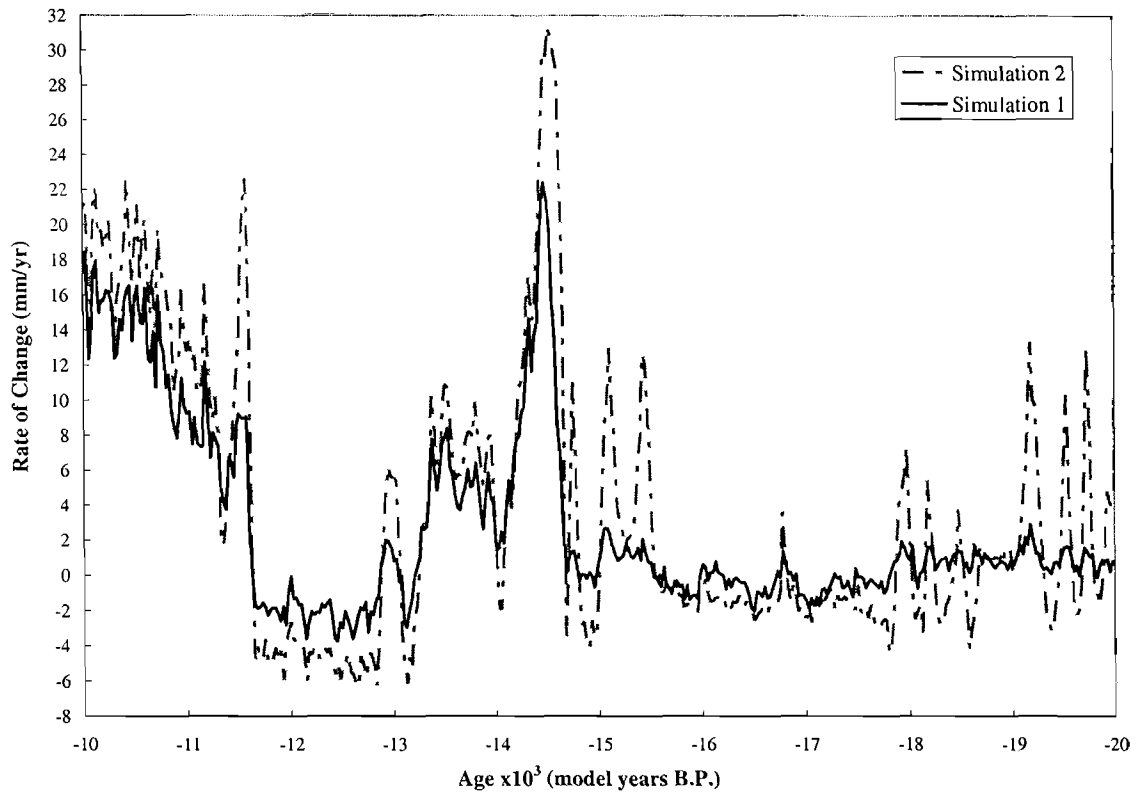


**Fig. 15.** Experiment 1 results. **a.** GISP2 was scaled by 40% for Simulation 1 and 50% for Simulation 2. The relative timing of ice buildup and decay is the same for both simulations; however, the magnitudes of changes are different. Ice-volume buildup is gradual for the glacial period followed by an abrupt termination. The LGM in these simulations does not end until about 14,700 model years, which is concurrent with the onset of the Bölling warming in GISP2.



**Fig. 15.** Continued. **b.** In the first simulation, a meltwater pulse of 6 m s.l. equiv. is predicted between 14,675 and 14,050 model years in response to a 5.7 °C (scaled 40%) warming at the onset of the Bölling. During the same period, an 11 m jump is produced in the second simulation in response to a 7.1 °C warming (scaled 50%). Note that the meltwater pulse in these simulations marks the termination of the LGM.



**c**

**Fig. 15.** Continued. **c.** The rate of sea-level change predicted from the meltwater pulse between 14,675 and 14,050 model years is 22 mm/yr for the first simulation and 31 mm/yr for the second. Note that in both simulations, the first measurable ice-volume loss does not occur until the onset of the Bölling warming.

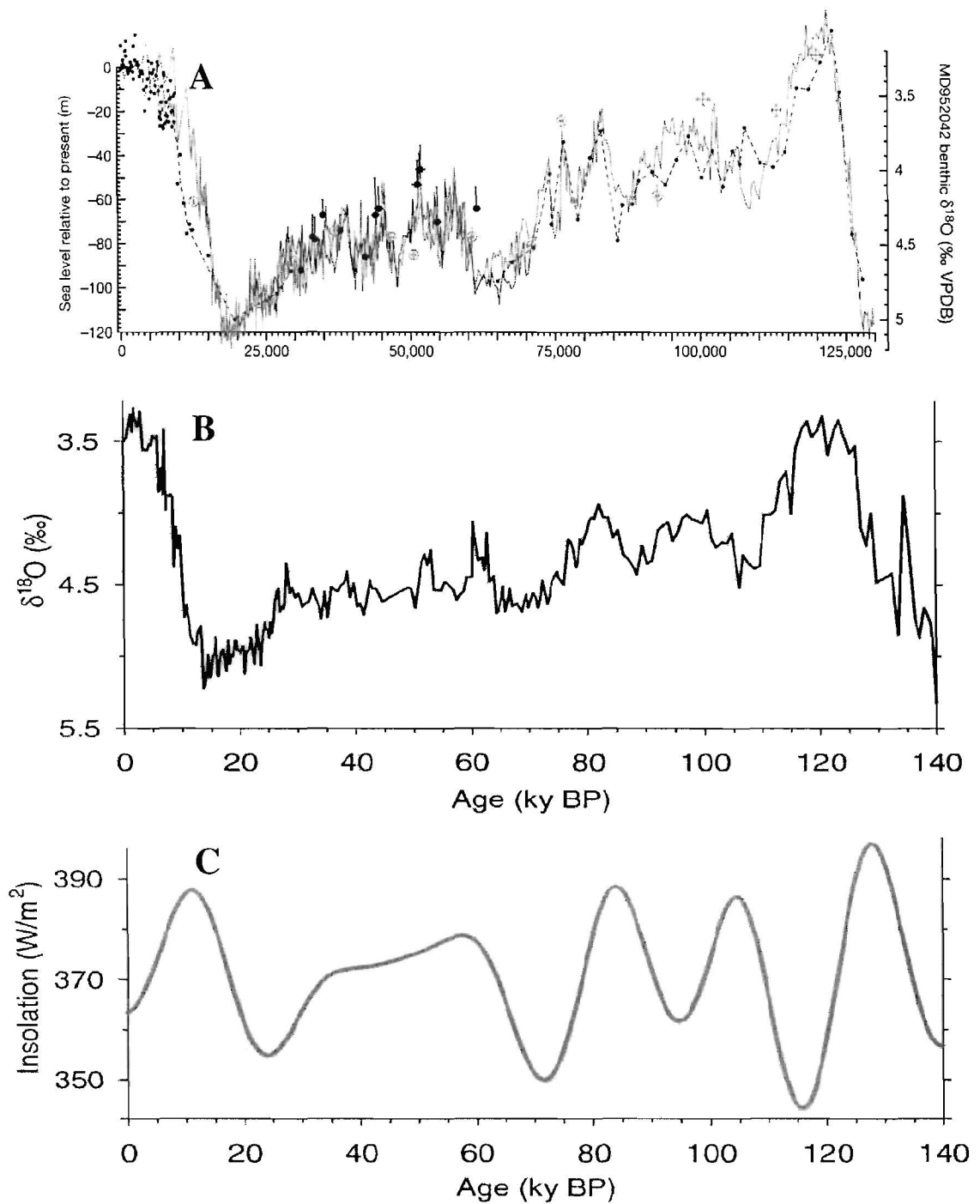
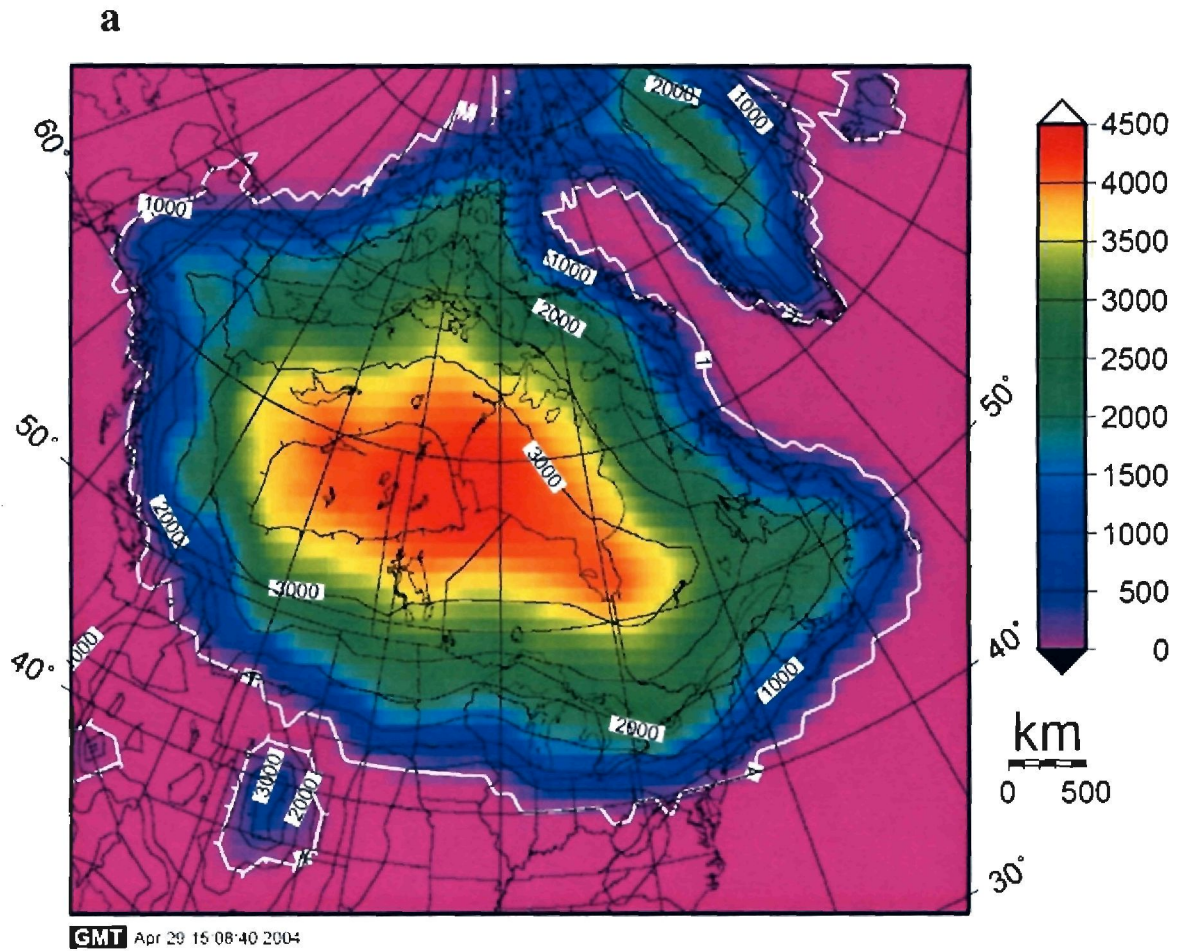


**Fig. 16.** Pattern of glaciation evident from paleoclimate indicators. A. Relative sea level derived from salinity changes in the Red Sea (Siddall *et al.* 2003). B. Benthic oxygen isotope record of East Pacific core V19-30 (Shackleton 1987). Ice-volume buildup through the last glaciation was gradual with an abrupt termination. The pattern is similar to that of July insolation changes for 65 °N latitude (Berger 1978).

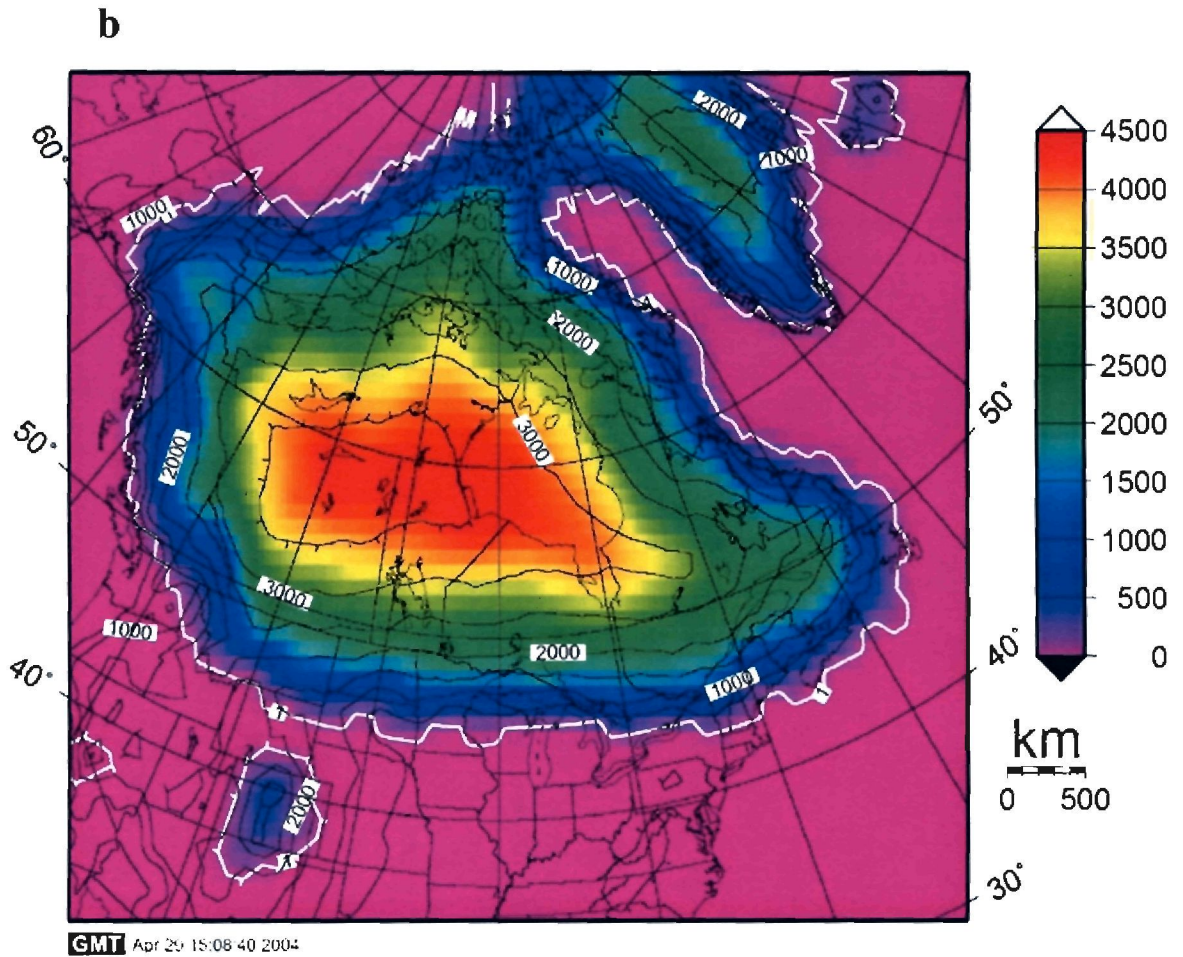
model years and the glacial termination does not start until -15,000 model years. The Laurentide LGM ice-cover is expansive, with a single dome west of Hudson Bay (Fig. 17a). There is not a distinction between the Cordilleran and Laurentide Ice Sheets, as they are merged. Alaska is largely ice free.

Figure 17b shows the configuration of the ice sheet immediately preceding the onset on the Bölling-Alleröd at -15,000 model years. The first significant ice-volume reduction occurs between -14,675 and -14,050 model years in response to the abrupt rise in temperature beginning at about 14,700 ice core years B.P. The peak rate of change during this interval is 31.37 mm/year (s.l. equivalence) centered at -14,525 model years. This event corresponds to a meltwater pulse whereby sea-level would rise 10.2 m over a period of 625 years. Figure 17c shows that the overall configuration of the ice sheet was not greatly affected by the pulse.

In response to mean-annual temperature depression during the Younger Dryas, ice-volume begins to increase at about -12,700 model years. Ice-buildup is followed by an abrupt warming starting at -11,650 model years. A meltwater pulse is generated with a peak discharge of 22.69 mm/year (s.l. equivalence) at -11,575 model years. Rapid deglaciation ensues from -11,000 and -8,000 model years with sea-level rise between 12 and 24 mm/year, or nearly as high as the first predicted meltwater pulse. The ice sheet is gone by -5,000 model years.



**Fig. 17.** Experiment 1 ice-sheet configurations. **a.** LGM reconstruction. The total ice volume over North America is 80 m (s.l. equiv.). In this reconstruction, the Laurentide and Cordilleran Ice Sheets are a single entity. Contour lines denote surface elevation, whereas as colors indicate ice thickness in meters.



**Fig. 17.** Continued. **b.** -15,000 model year reconstruction immediately preceding the initial Bölling warming. Total ice volume is 77 m (s.l. equiv.). The ice sheet is almost identical to that simulated at the LGM, with the exception of a minor retreat along the southeastern ice margin. Contour lines denote surface elevation, whereas as colors indicate ice thickness in meters.



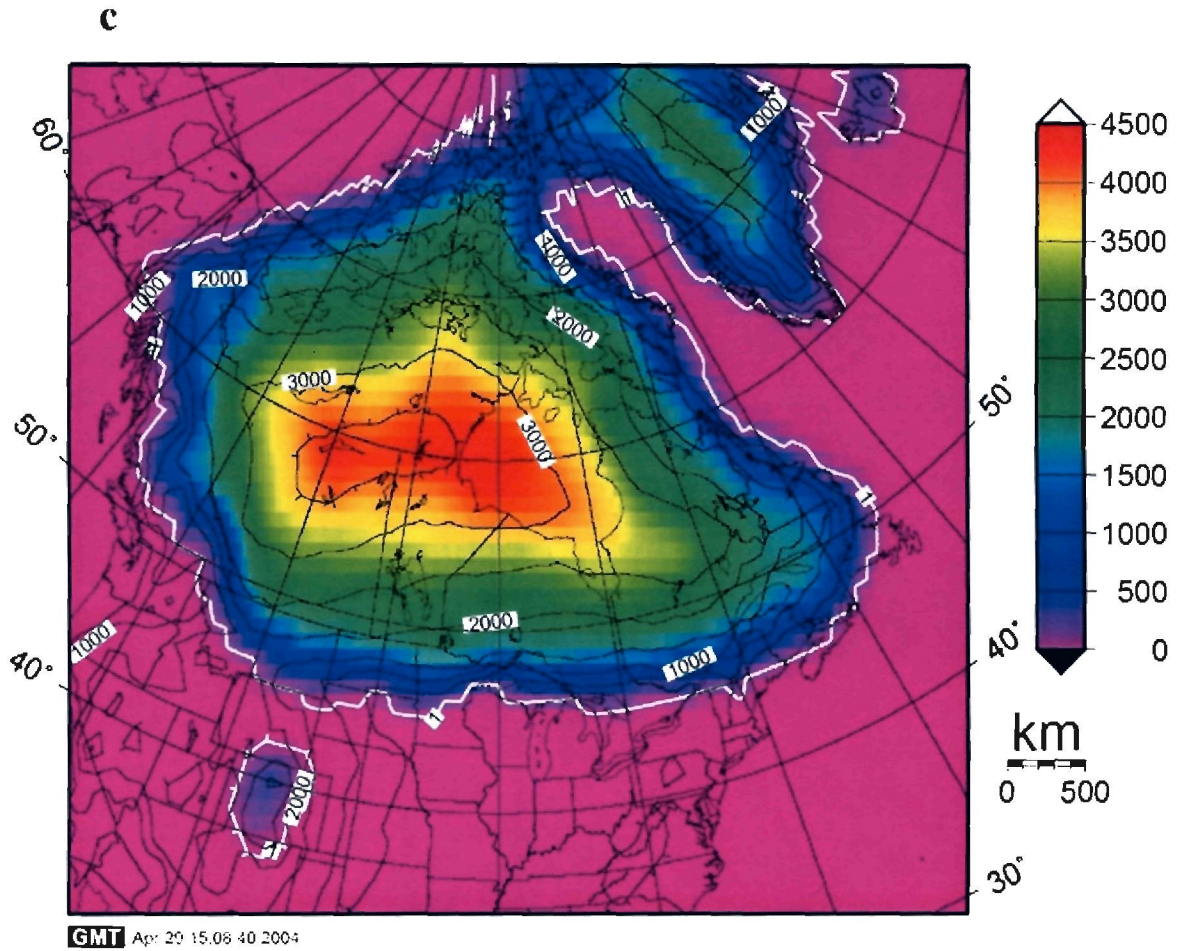


**Fig. 17.** Continued. **c.** -14,000 model year reconstruction immediately after the initial Bölling warming. Total ice volume is 66.5 m (s.l. equiv.). The model predicted a meltwater pulse of 10.5 m between -14,700 and 14,000 model years in response to the 6°C Bölling temperature spike. The ice sheet still retains an LGM-like configuration. Contour lines denote surface elevation, whereas as colors indicate ice thickness in meters.

## 5.2 Discussion

Experiment 1 shows a simulated meltwater pulse from the LIS in response to the elevated temperature during the onset of the Bölling. However, some aspects of this experiment afford problems. First, the Laurentide and Cordilleran Ice Sheets are not separate entities at the LGM. Instead, the ice sheets are merged and a single dome is formed west of Hudson Bay. Although, their margins may have converged along the southeast-northwest-trending ice-free corridor east of the northern Rocky Mountains, these ice sheets are commonly understood to have remained basically independent masses throughout the last glaciation. This divergence between geology and the modeled ice sheet probably occurs because the simple climatology model used by the UMISM is not robust. The model does not incorporate a Global Circulation Model (GCM); therefore it does not consider heat advection due to atmospheric circulation.

In the modern climate system, air pushing eastward from the Pacific encounters the extensive, high-elevation mountain belts of western North America and is subsequently diverted to the north and south (Fig. 18). The result is a perturbation in the polar jet stream whereby a semi-permanent Rossby wave forms over the North American continent. Relatively warm sub-tropical air is forced over Alaska, where it proceeds southeast along the Rocky Mountain front. To the east is the Hudson Bay region of the Canadian Shield where there is significant snow-and-sea-ice cover for much of the year. The elevated albedo over this broad swath of land causes a steep temperature gradient between the overlying cool Arctic air, and the warm sub-tropical air to the south. To this end, a positive albedo feedback facilitates southward depression of the polar jet stream.

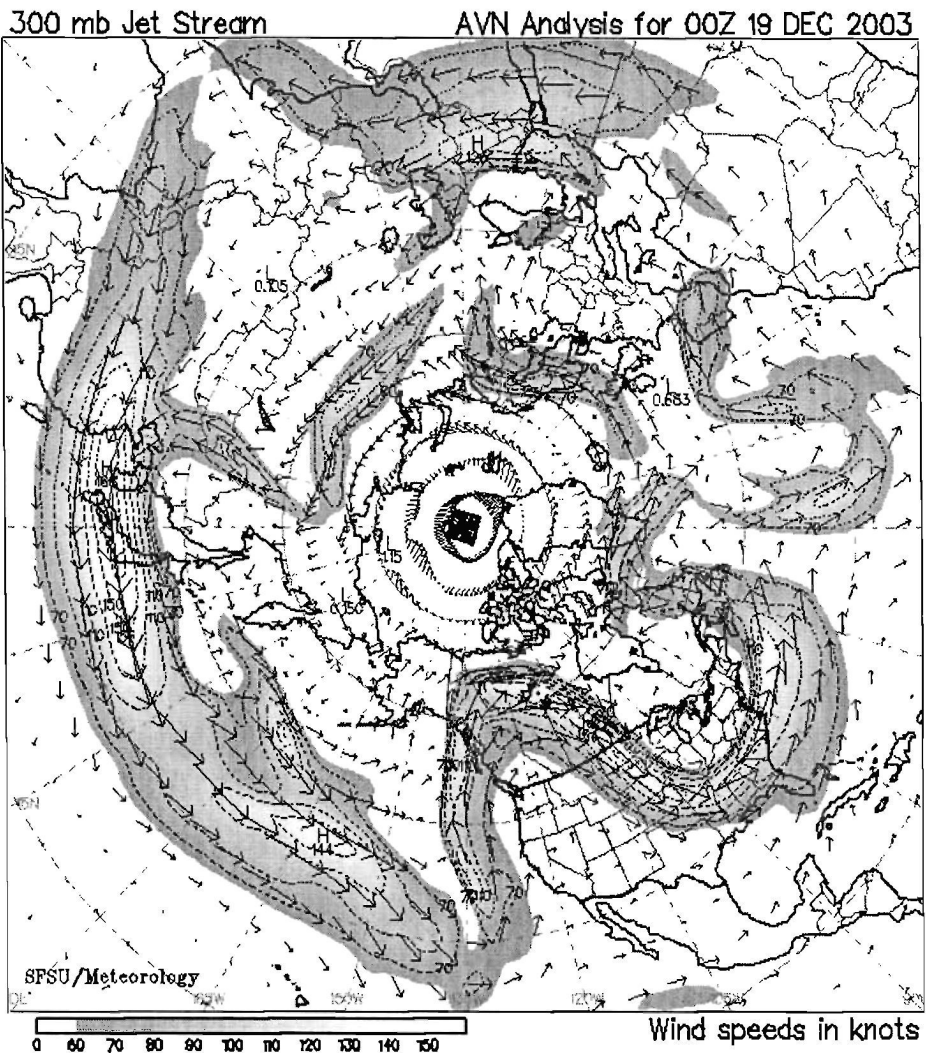


**Fig. 18.** Typical winter configuration of the polar jet stream over the Northern Hemisphere. High elevation topographic relief in western portion of the North American continent deflects air moving eastward across the Pacific. The result is a Rossby wave that transports warm air to high latitudes in the west and cold air to mid latitudes in the east.



In addition, warm maritime air provides a buttress along the eastern seaboard whereby the jet is forced northeastward over the North Atlantic and into Scandinavia. The net affect is a persistent trough of Arctic air over North America that penetrates the mid-latitudes. Therefore, warm air pouring southeastward from Alaska affords a zone of ablation that would inhibit the coalescence of the Laurentide and Cordilleran Ice Sheets.

A second major problem is evident from Experiment 1 results. The predicted deglacial chronology does not match that known from sea-level records. Instead of a gradual decrease in ice volume following a distinct LGM at around 19,000 calendar years B.P., the model shows the persistence of an LGM-like configuration until about -14,700 model years, or the onset of the Bölling. By this time sea level at Barbados had already risen about 30 m above the LGM sea-level lowstand (Fairbanks 1989; Bard *et al.* 1990). Furthermore, evidence for an early deglaciation comes from the Great Lakes region (Lundqvist and Saarnisto 1995) and the coast of New England (Borns *et al.* in press 2002) where much of the periphery of the LIS had retreated significantly from its LGM margin before the onset of the Bölling.

The incorrect deglacial chronology of the modeled ice sheet is a product of the GISP2 climate forcing. Instead of a well-defined LGM, there is a gradual cooling that peaks at about 32,000 ice core years B.P. The first major warming evident in GISP2 is that of the Bölling. This pattern of climatic change is in contrast to moraine chronology (Lundqvist and Saarnisto 1995) that indicates recession of the Laurentide and Scandinavian ice sheets began about 18,000  $^{14}\text{C}$  years B.P. Furthermore, the GISP2 record is also incompatible with the deglacial history recorded in ice cores from East Antarctica (Fig. 11). Here the LGM occurred between 17,000 and 19,000 ice core years

B.P. and was followed by a steady climatic warming. Moreover, there is a striking resemblance between temperature change recorded in Antarctica and global sea-level reconstructions (Fig. 19). One might argue that a signal of global climatic change is found in Antarctica, but that from Greenland is somehow incomplete or inaccurate.

High-amplitude climatic changes in GISP2 (*e.g.*, the severe LGM and Younger Dryas cooling) might reflect a complex and unresolved seasonality, whereby temperature is unevenly weighted between summer and winter (Denton *et al.* in press 2005). As evidence for seasonality, the Younger Dryas temperature depression appears equally low as that of the LGM in the GISP2 record, but glacier moraine records indicate that ice sheets at the time were still retreating (Denton *et al.* in press 2005) and sea level was rising (*e.g.*, Fairbanks 1989; Bard *et al.* 1990; Hanebuth *et al.* 2000; and others). Furthermore, beetle remains show that winter months in the British Isles just before the Bölling transition were between -20 and -25 °C whereas summers reached to 30 – 35 °C warmer (Atkinson *et al.* 1987). These results indicate that a continental climate, probably linked to extensive sea-ice cover, existed over the North Atlantic region during cold stadial winters. With the onset of the Bölling, summer temperatures warmed by 7 to 8 °C whereas winter temperatures jumped by about 25 °C (Atkinson *et al.* 1987). Moraine/snowline records in Scoresby Sund, East Greenland corroborate that extreme temperature depressions observed in Greenland ice cores may have been heavily weighted towards the winter season. Denton *et al.* (in press 2005) calculated, based on moraine deposits, that a mean summer temperature depression of less than about 5 °C was responsible for a snowline drop of ~600 m during the Younger Dryas. However, the GISP2 ice-core recovered at summit, Greenland shows a 15 °C mean-annual-temperature

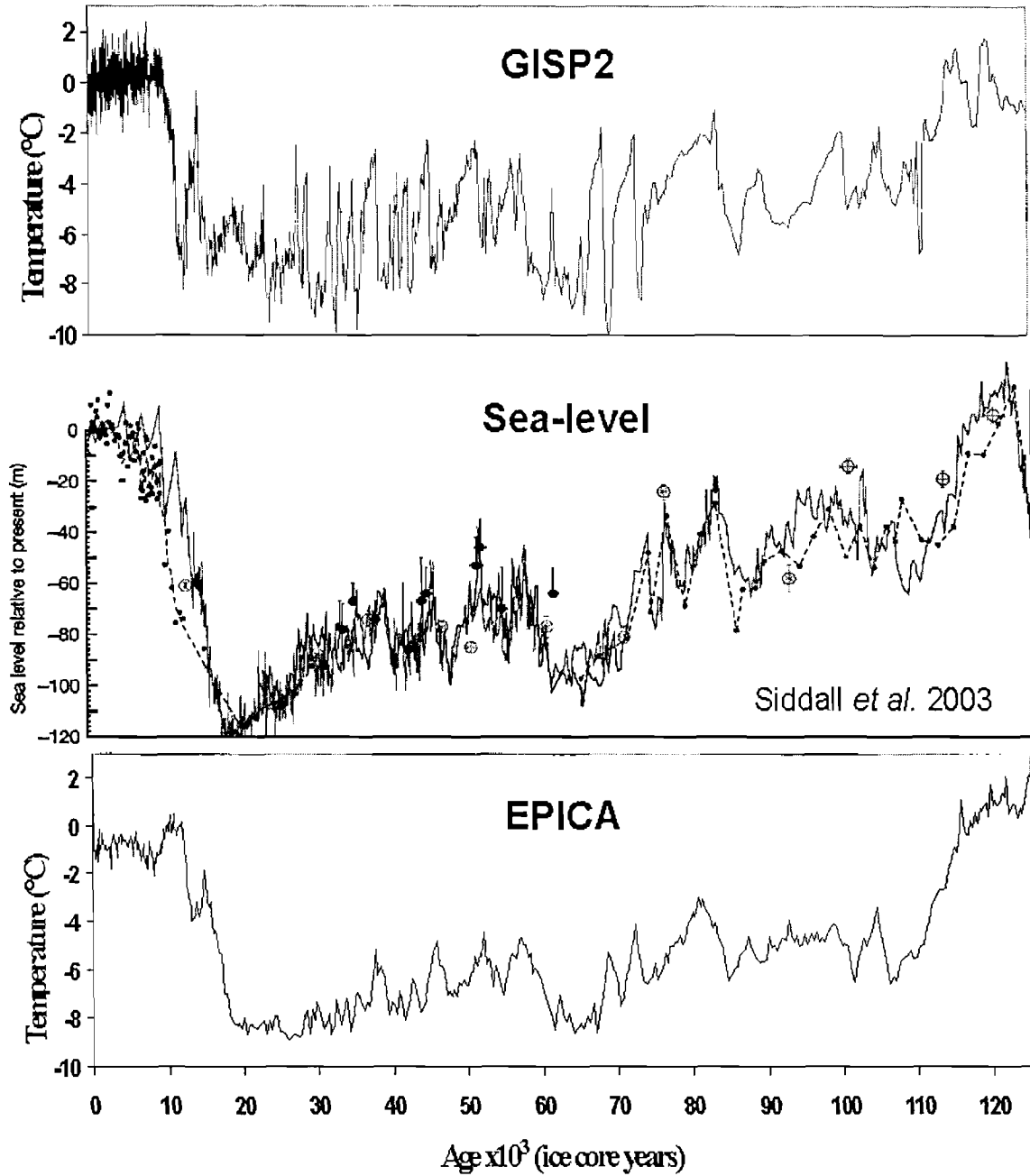


**Fig. 19.** Comparison of paleoclimate records. The pattern of glaciation is nearly identical between the sea level record from the Red Sea (middle) (Siddall *et al.* 2003) and the EPICA Dome C record of mean-annual temperature changes in Antarctica (bottom). Note the clear glacial termination at about 19,000 years. The Greenland GISP2 record (top) is somewhat dissimilar in that the LGM appears to reach a maximum at about 30,000 years.

change for the same period (Severinghaus *et al.* 1998). In effect, the geologic record appears to show changes dominated by weak summer temperature variations whereas the ice core record shows high-amplitude oscillations skewed by high-magnitude winter changes.

Thus, because of unresolved seasonality, the 23 °C LGM mean-annual temperature drop recorded by GISP2 glaciates the earth in the degree-day mass-balance scheme used by the UMISM. A realistic ice sheet is attained by scaling down the amplitude of the GISP2 signal, thereby crudely approximating the more modest summer temperature changes that probably actually occurred. Coincidentally, when scaled to 40%, GISP2 LGM mean-annual temperature depression is between 8 and 10 °C, similar in magnitude to that of the Antarctic cores (Fig. 20).

In an attempt to reconcile problems with the GISP2 experiment, I developed an experiment whereby the LIS would be reconstructed by forcing model climate with a record from Antarctica. I chose to use the EPICA Dome C core (EDC2 chronology), primarily because the deglacial chronology closely matches that of sea-level records (Shackleton 1987; Siddall 2003). Furthermore, the ~1.2 °C warm peak recorded by EPICA immediately preceding the Antarctic Cold Reversal (ACR) could potentially produce a small meltwater pulse. Here I equate these Southern Hemisphere events to the Bölling and Younger Dryas of the Northern Hemisphere respectively for the purpose of modeling; however, I recognize that climatic change between the hemispheres may in reality be asynchronous (*e.g.*, Blunier *et al.*, 1998).

It is unlikely that MWP 1A could be derived from the modest warm spike preceding the ACR in the EPICA temperature record. This is because a 10.2 m

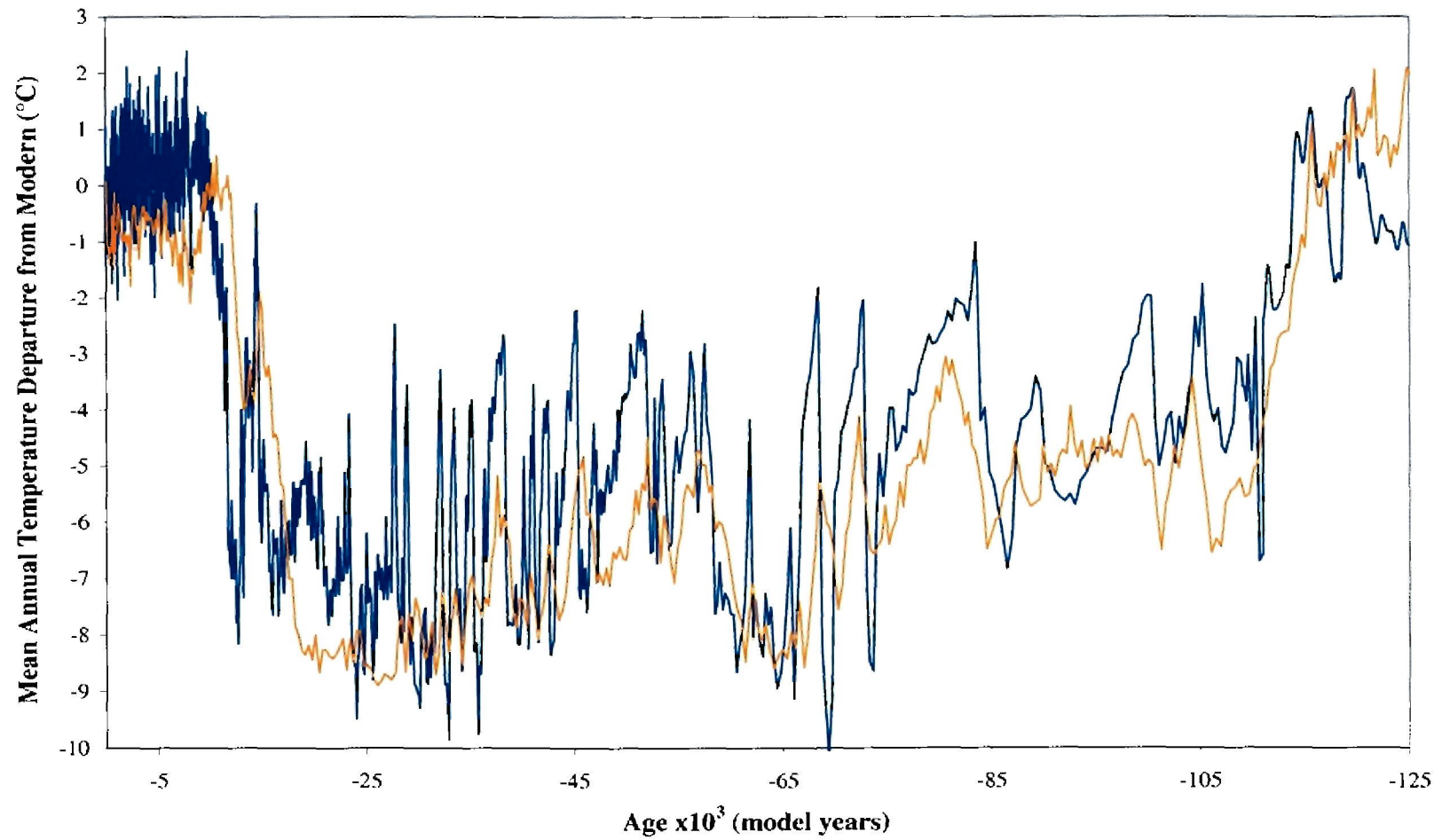


**Fig. 20.** The EPICA Dome C (EDC-2 timescale) and scaled GISP2 records. Refer to Figure 11 for comparison between Northern and Southern Hemisphere ice-core chronologies.

meltwater pulse resulted from the  $\sim 7$  °C (scaled 50%) GISP2 warming at the onset of the Bölling in Experiment 1; therefore, I decided to run two additional simulations whereby the EPICA warming would be artificially enhanced to reflect a modern climate. In effect, the model would test what magnitude of warming might be necessary to produce MWP 1A. For the second simulation, a single data point at 14,775 ice core years B.P. was changed from  $-1.9$  °C to  $0$  °C (modern value). In the third experiment, I let a modern climate persist for 300 model years centered around 14,814 ice core years B.P. 300 years is the duration of MWP 1A inferred from the Sunda Shelf (Hanebuth *et al.* 2000). These modifications, although arbitrary, are meant to simulate the Bölling climatic warm pulse (Fig. 21).

### 5.3 Experiment 2

The first stage of this experiment was to develop a realistic LGM ice sheet. In order to prevent the coalescence of the Laurentide and Cordilleran Ice Sheets, I emplaced a zone of negative mass balance along the Rocky Mountain front (Fig. 22). This in effect simulated the topography-induced Rossby wave that divides warm sub-tropical from polar air over North America. I then let the model run through a full glacial cycle to build ice to an LGM configuration. Southern ice margins were constrained slightly to match known terminal positions (Lundqvist and Saarnisto 1995).

Figure 23 shows the resultant Northern Hemisphere LGM configuration. Total s.l. equiv. ice volume is  $\sim 82$  m ( $\sim 72$  m LIS;  $\sim 4$  CIS;  $\sim 6$  GIS). It was difficult to decide on an appropriate configuration of the CIS and Alaska ice caps; therefore, another

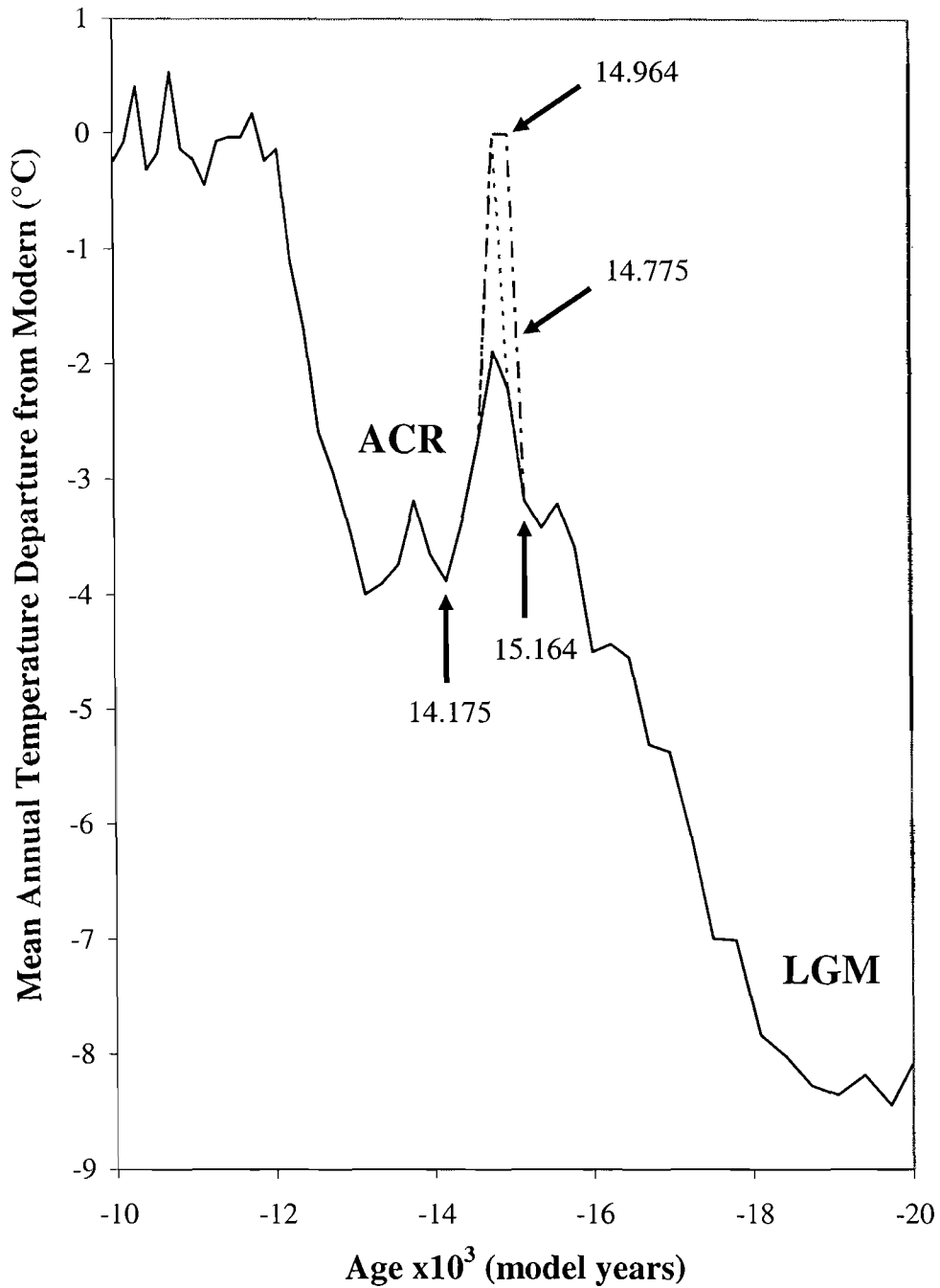


**Fig. 21.** The EPICA EDC2 record formatted for the UMISM showing from 20,000 to 10,000 ice core years B.P. Simulation 1 used the input unchanged. In the second test, a single data point was changed to the 0 °C modern climate baseline at 14,775 ice core years B.P. The third simulation was similar to the second; however, the modern climate was held for 300 years starting at 14,964 ice core years B.P. 14,175 ice core years B.P. marks the beginning of the Antarctic Cold Reversal (ACR).

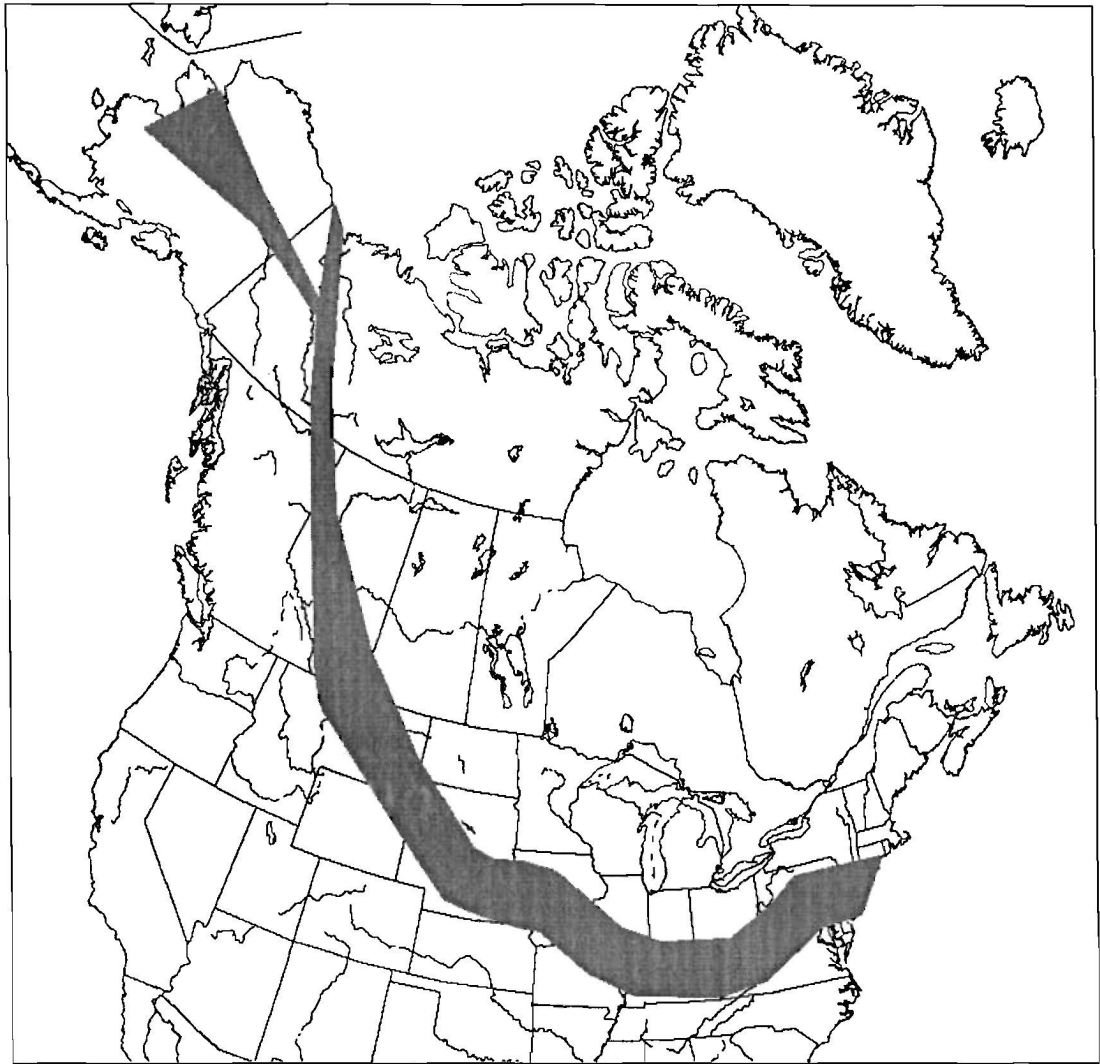


**Fig. 22.** Map-plane mass-balance modifications used in Experiment 2. The area shaded in red represents a zone of net ablation. Without this enhancement, the Laurentide and Cordilleran Ice Sheets merge unrealistically.



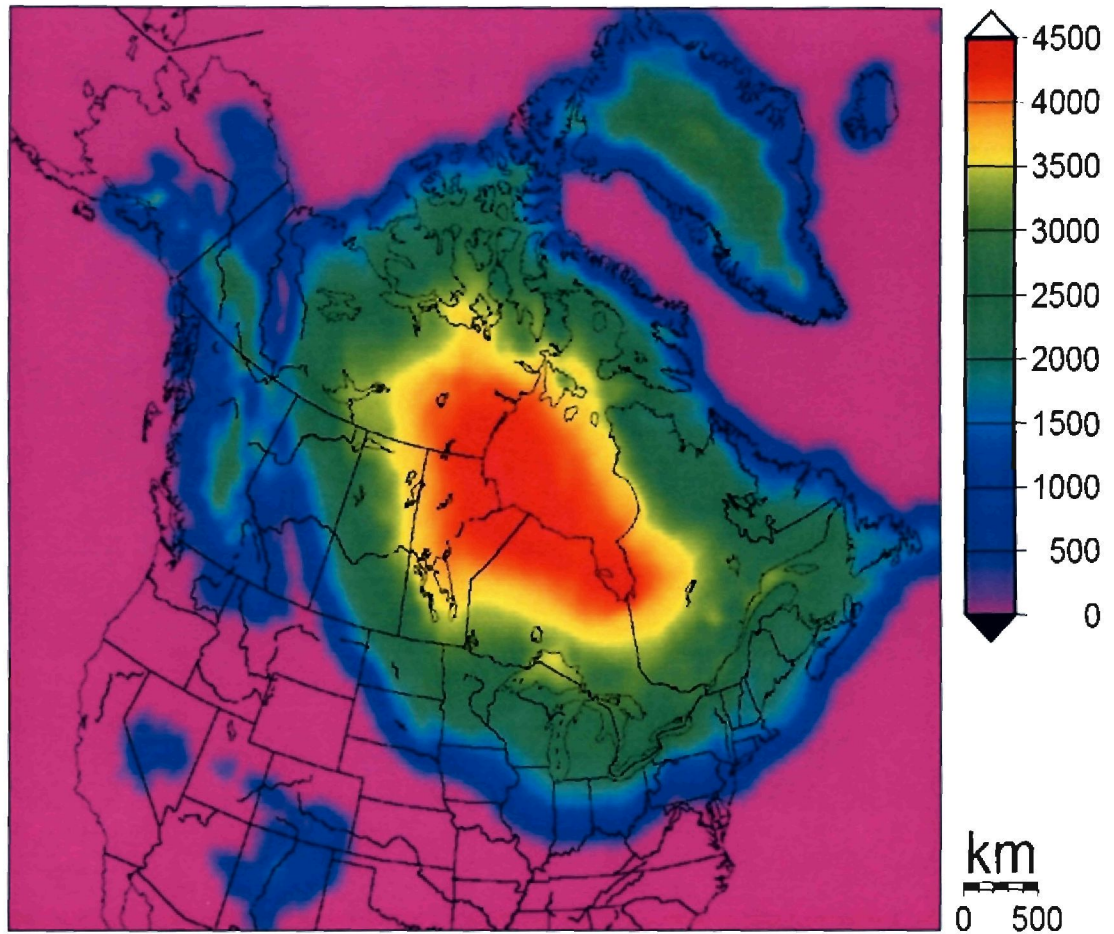


**Fig. 23.** Experiment 2 LGM ice-sheet configuration. Mass-balance adjustments were used to prevent the coalescence of the Laurentide and Cordilleran Ice Sheets. The LIS volume is  $\sim 72$  m (s.l. equiv.). Colors indicate ice thickness in meters.

baseline was reconstructed to include only the Laurentide and Greenland Ice Sheets (Fig. 24).

The model was then set to continue through to the Holocene, or -10,000 model years using the unmodified EPICA temperature input. Refer to Figures 25a and b for model results. In the first simulation, a distinct meltwater pulse is not readily evident; however, increased melting is predicted between -15,150 and -14,425 model years with a 12.2 mm/yr peak rate of change at -14,775 model years (Fig. 25b). During this interval, the sea-level equivalent ice volume changed from 69.6 to 62.4 m, or a rise of 7.2 m. In the second simulation, whereby a single data point was elevated to the modern climate, an 8.1 m meltwater pulse is predicted between -15,150 and -14,500 model years, with a 23 mm/yr peak rate of change at -14,775 model years. In the third simulation, a change in slope is evident between -15,050 and -14,550 model years wherein ice volume jumps 10.5 m sea-level equivalence with a maximum rate of change is 24.5 mm/yr at -14,950 model years. The third test produced the largest meltwater pulse; accordingly, the ice margin of the LIS retreated significantly (Figs. 26a, b).

#### *5.4 Discussion*

A meltwater pulse was produced from the LIS in all three simulations using the EPICA EDC-2 climate input to drive the model; however, the only significant sea-level jump (10.5 m ice volume s.l. equiv.) is that which resulted from imposing a modern climate over the ice sheet for 300 model years immediately preceding the ACR. The duration of this event (500 model years) is compatible with that of MWP 1A observed at

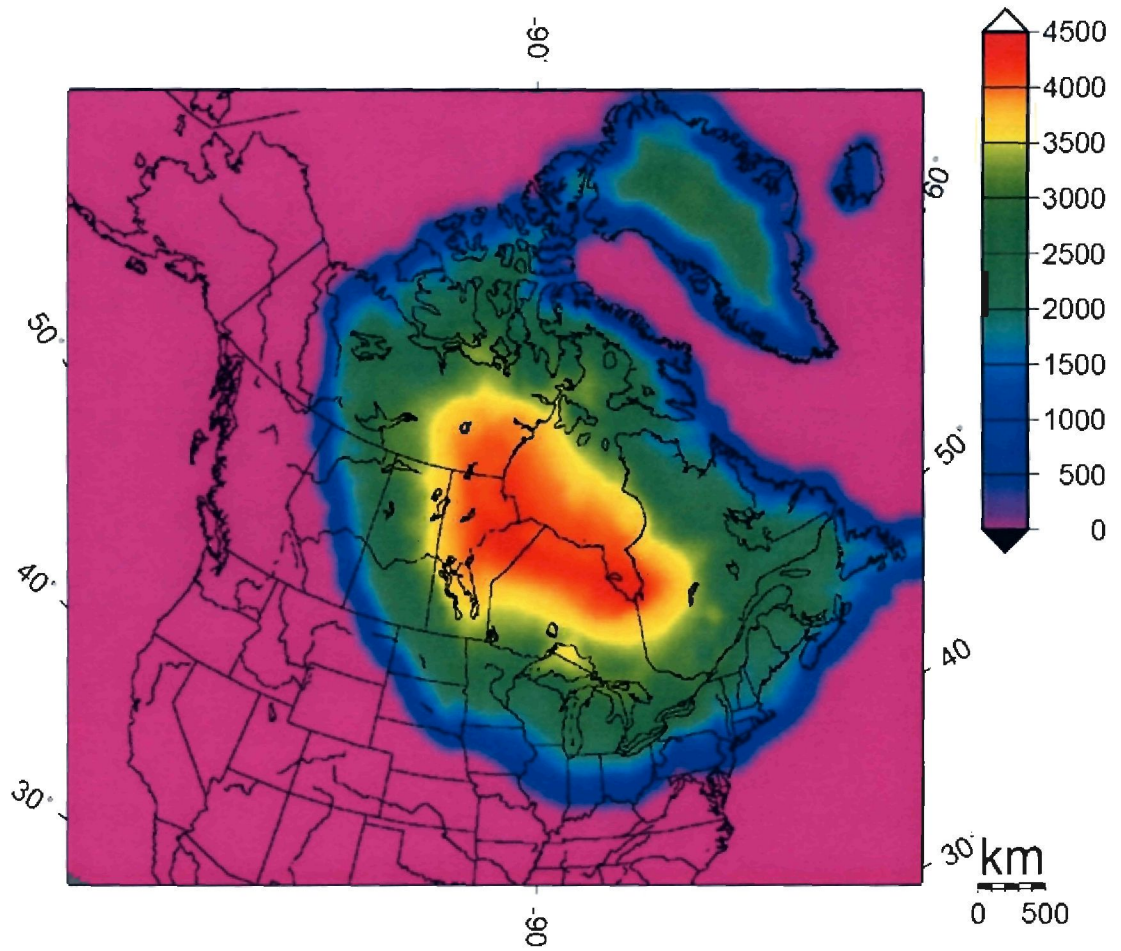


**Fig. 24.** Experiment 2 LGM ice-sheet configuration with mass-balance adjustments that prevented growth of ice over the Cordilleran. The LIS volume is ~72 m (s.l. equiv.). Colors indicate ice thickness in meters.

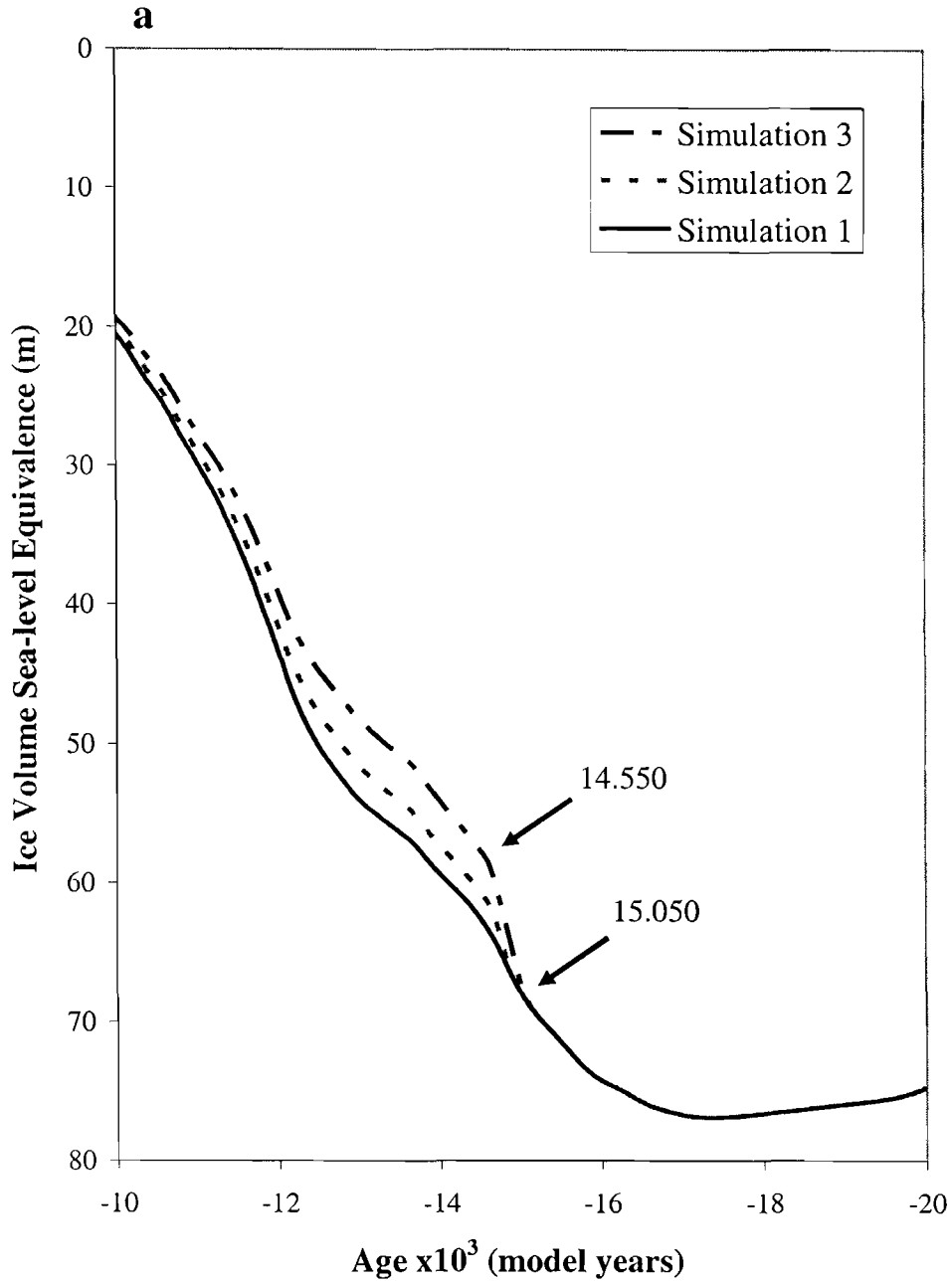


**Fig. 25.** Experiment 2 results. **a.** A prominent meltwater pulse of 10.5 m s.l. equiv. between 15,050 and 14,550 model years is predicted for the third simulation whereby climate is arbitrarily warmed to modern values for 300 model years.

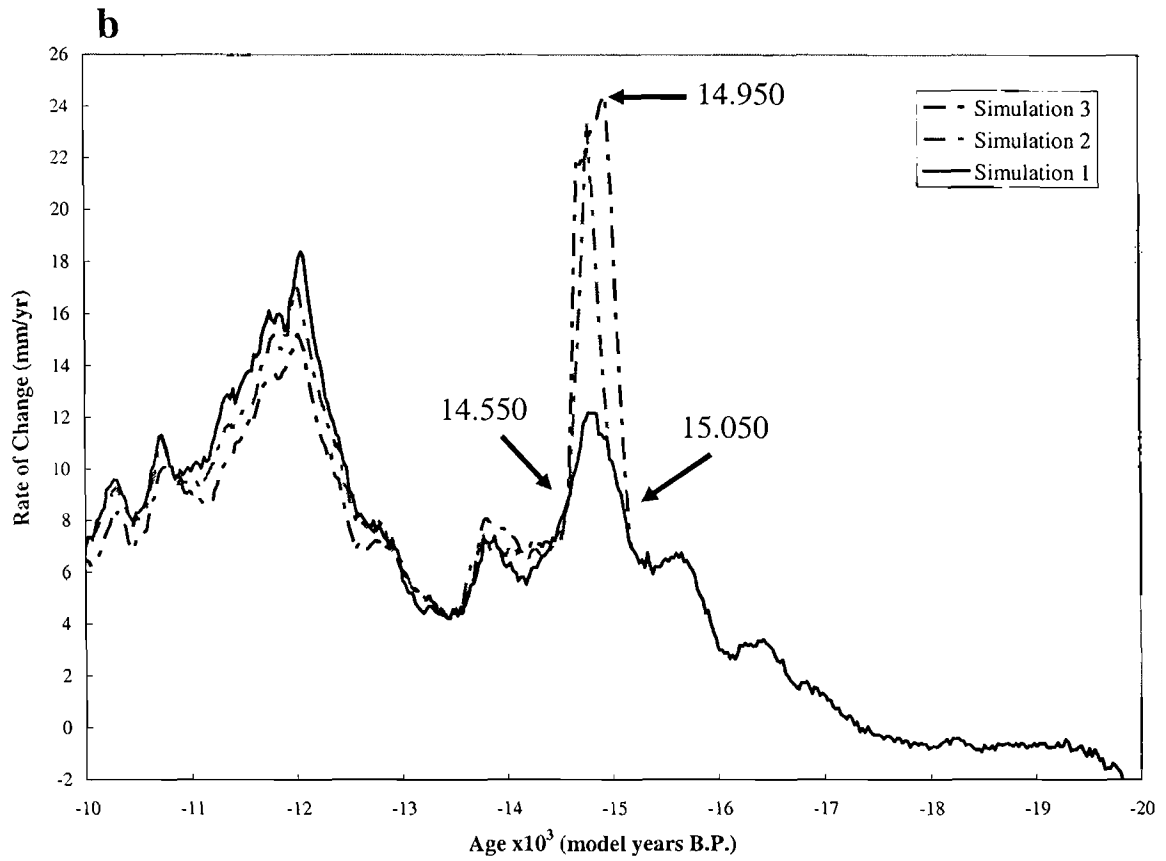


**Fig. 25.** Continued. **b.** A prominent meltwater pulse of 10.5 m s.l. equiv. between -15,050 and -14,550 model years is predicted for the third simulation whereby climate is arbitrarily warmed to modern values for 300 model years. The peak rate of sea-level change is 24.5 mm/yr at -14,950 model years.

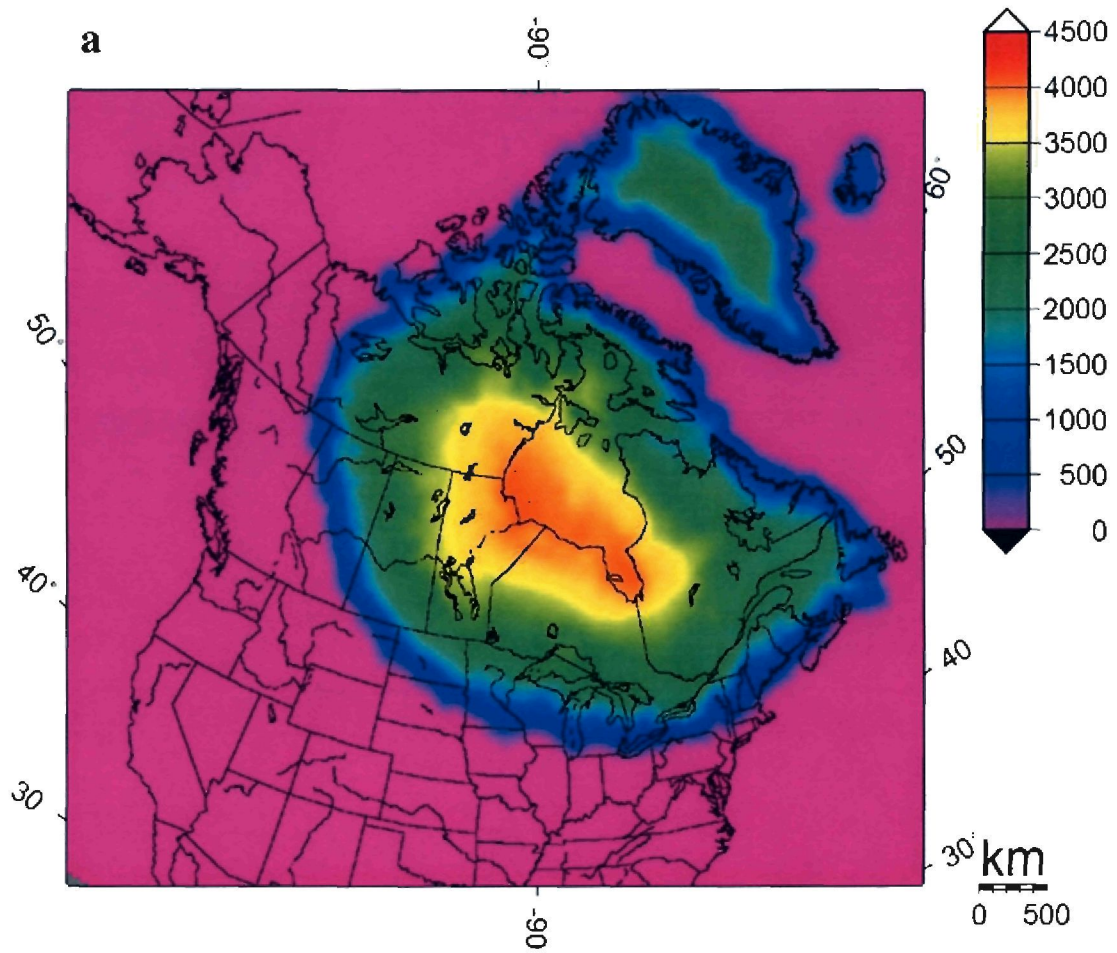


**Fig. 26.** Experiment 2 ice-sheet configurations. **a.** -15,000 model years. The LIS volume is 67 m (s.l. equiv.). Colors indicate ice thickness in meters.



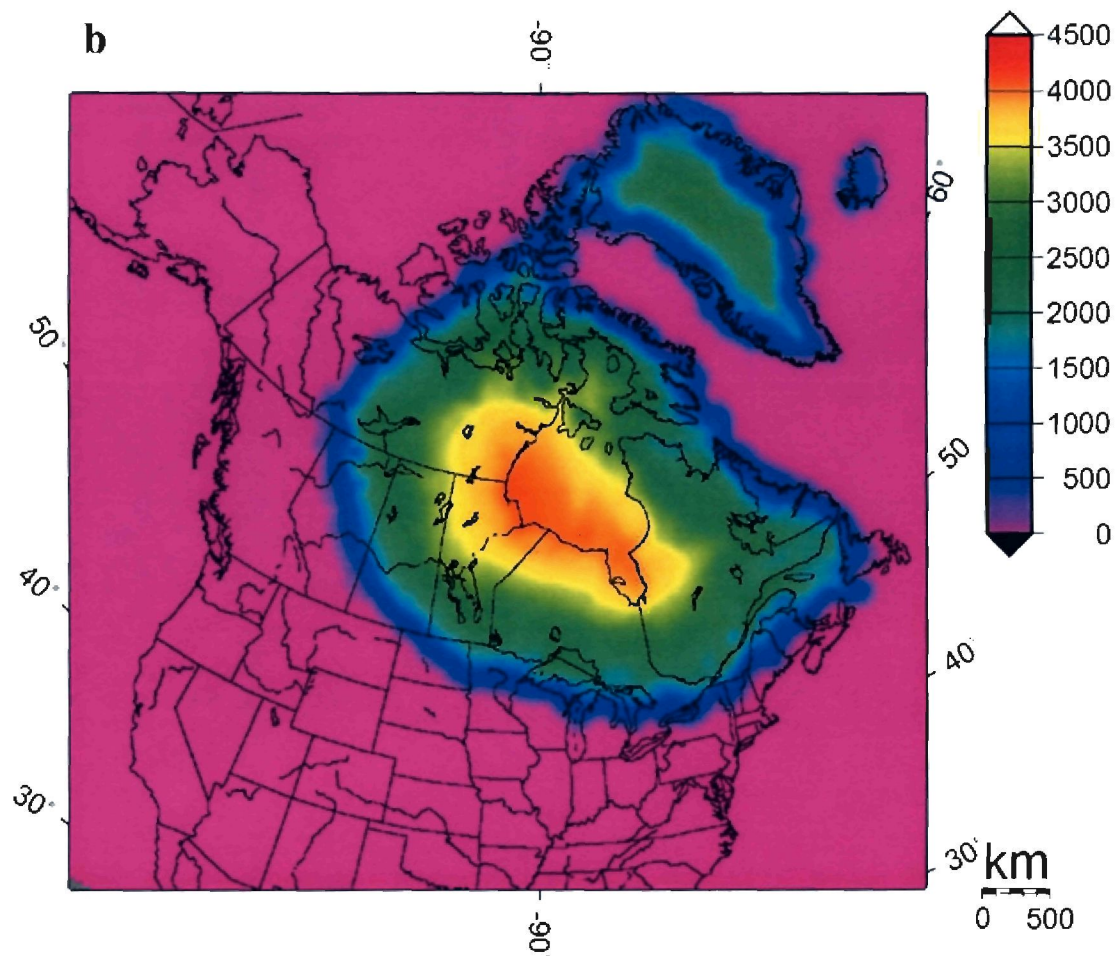


**Fig. 26.** Continued. **b.** -14,600 model years. The LIS volume is ~66.5 m (s.l. equiv.). Imposing a modern climate for 300 years (a mean-annual temperature elevation of 3.1 °C from the pre-ACR baseline) resulted in a 10.5 m meltwater pulse between -15,050 model years and -14,550 model years. Colors indicate ice thickness in meters.

Barbados (less than 1000 calendar years) and the Sunda Shelf (about 300 calendar years). The 25 mm/yr peak rate of s.l. equiv. change is comparable to that estimated for MWP 1A at Barbados (~27 mm/yr); however, the predicted value is less than half that estimated from Sunda Shelf data (53 mm/yr).

The timing of the simulated meltwater pulse using EPICA EDC-2 (-15,100 to -14,400 model years) is earlier than that observed at Barbados (~14,700 and 13,800 calendar years B.P.) but consistent with the timeframe estimated for MWP 1A observed at the Sunda Shelf (~15,300 to 14,280 calendar years). In contrast, the meltwater pulse predicted in Experiment 1 using the GISP2 timescale occurred between -14,675 and -14,050 model years. It is necessary to emphasize that temporal events predicted by the UMISM are strongly dependent upon the chronology of the temperature input. Figure 11 illustrates that ice-core chronologies are not absolute and differ considerably; therefore, precise timing of MWP 1A cannot be deduced from these results.

The magnitude of the meltwater pulse predicted in Experiment 2 (10.5 m) is much smaller than that estimated from Barbados (19 – 24 m) (Fairbanks 1989; Bard *et al.* 1990), the Sunda Shelf (16 m) (Hanebuth 2000) and elsewhere in the Caribbean Atlantic (13.5 m) (Blanchon and Shaw 1995). I stress that an artificial change to the climate forcing was necessary to obtain these results. Furthermore, even by arbitrarily rising the mean-annual temperature to the modern baseline for 300 years, the model only barely produced a meltwater pulse. Therefore, it is possible that the Scandinavian Ice Sheet lost a proportional amount of ice volume (2 – 4 m) to that of the Laurentide in response to the Bölling warming. Alternatively, MWP 1A may have been considerably less dramatic than previously inferred.



Both experiments indicate that it is barely possible for MWP 1A to have come from the LIS. But where did the meltwater discharge? Figures 27a and b show basal water thickness (a proxy for ice streams) for the ice sheet before and after the meltwater pulse. Major ice streams were generated by the model in the Hudson Strait, Gulf of St. Lawrence, along the southern ice sheet margin and in the northwestern Canadian Arctic. Figure 28 shows that about 40% (~0.09 Sv) of the additional meltwater produced during MWP 1A came from the southern sector of the LIS and therefore would have discharge through the Mississippi into the Gulf of Mexico. About 25% (~0.06 Sv) of the meltwater drained into the North Atlantic east of the Appalachian Mountains. In contrast, 30% (~0.07 Sv) of the elevated discharge entered into the Arctic Ocean. Discharge increased into the Hudson Strait and Labrador Sea was negligible (<0.01 Sv).

These results are compatible with the influx of  $\delta^{16}\text{O}$  measured in cores from the Gulf of Mexico (Laventer *et al.* 1982) and the Bermuda Rise (Keigwin *et al.* 1991); they are also consistent with the lack of oxygen isotopic freshening during MWP 1A measured in a core from the Hudson Strait (Andrews *et al.* 1994). The elevated discharge predicted through the Gulf of St. Lawrence is inconsistent with the lack of evidence for increased  $\delta^{16}\text{O}$  into that region (Keigwin and Jones 1995).

Contrary to the assumption that a Laurentide-source MWP 1A would have to come from the southern margin of the ice sheet (Clark *et al.* 1996), the UMISM predicts that increased discharge occurred along much of its periphery. A substantial discharge of freshwater into the Arctic Ocean (~0.07 Sv) might explain anonymously high  $\delta^{18}\text{O}$  values found in Atlantic Ocean deep-sea cores reviewed by Clark *et al.* 1996. But again, the largest meltwater pulse generated by the UMISM was only 10.5 m s.l. equiv. and that

only by artificially warming climate. It is possible that discrepancies noted by Clark *et al.* 1996 exist because the magnitude of MWP 1A has been overestimated or that the extreme sea-level jump did not occur at all.

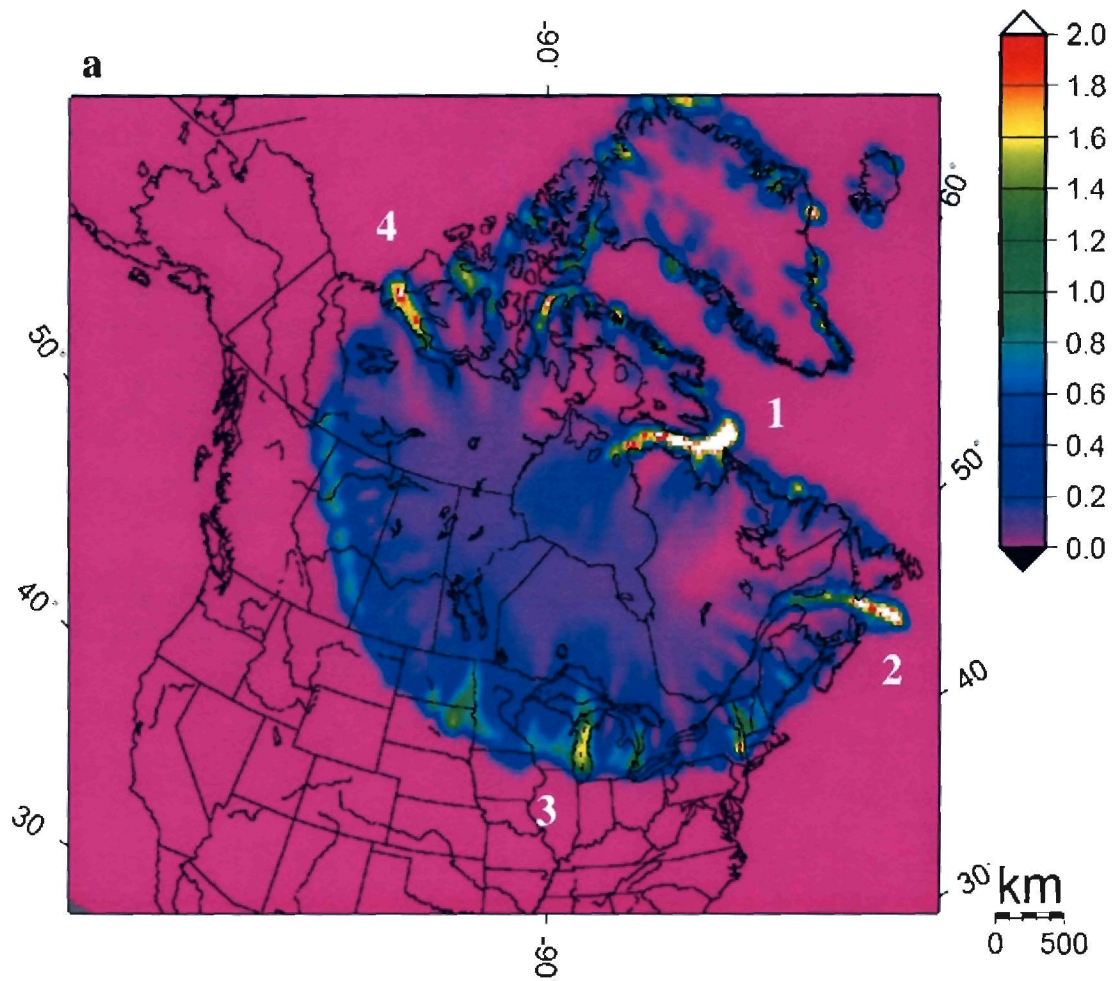


**Fig. 27.** Basal water thickness (in meters). **a.** At -15,000 model years, or immediately before the predicted meltwater pulse. Significant basal water buildup is indicative of increased sliding; therefore, these results can be used to infer the location of ice streams. The largest predicted ice stream (1) follows the Hudson Strait and drains into Labrador Sea; another significant ice stream (2) occupies the Gulf of St. Lawrence. Increased sliding is also evident along the southern margin of the ice sheet (3) and also in the northwestern Canadian Arctic (4).

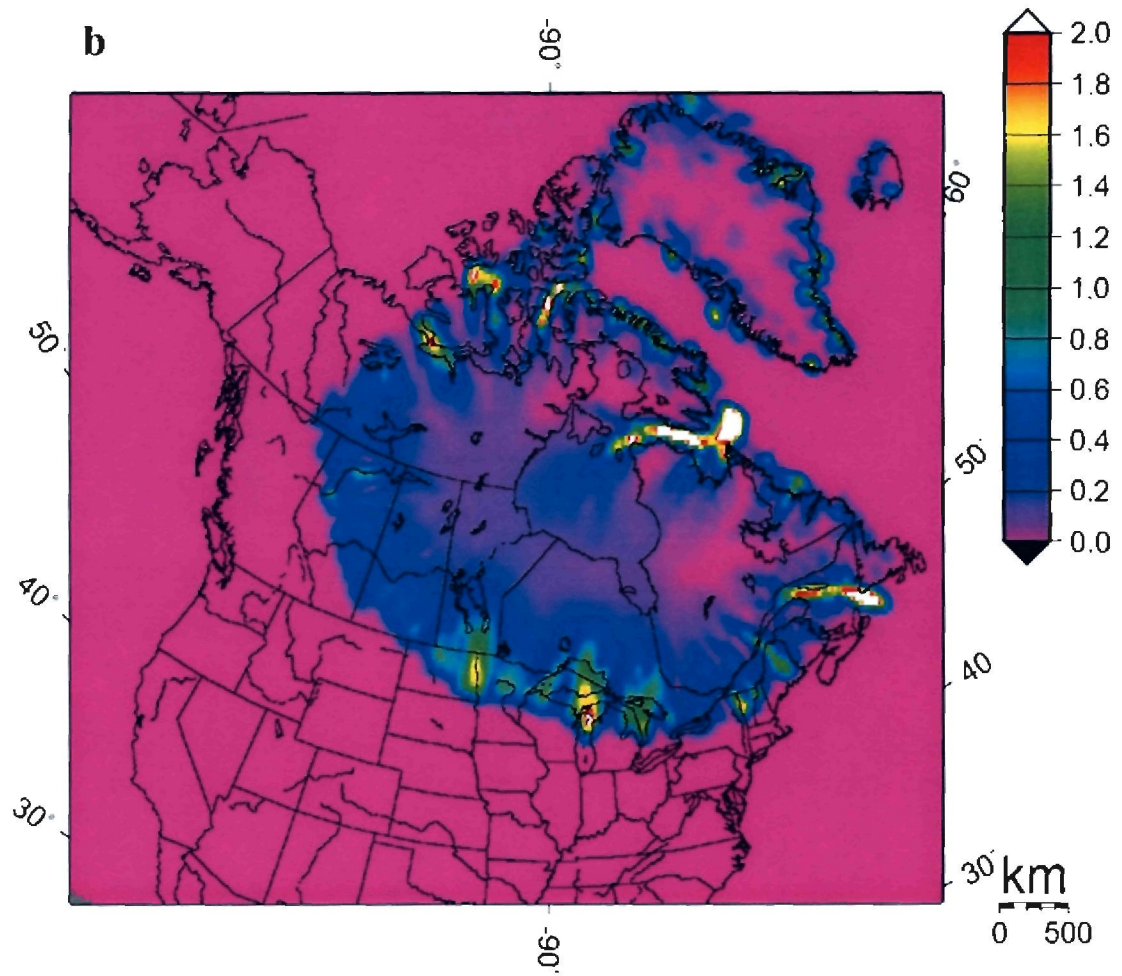


**Fig. 27.** Continued. **b.** At -14,600 model years, or just after the predicted meltwater pulse.

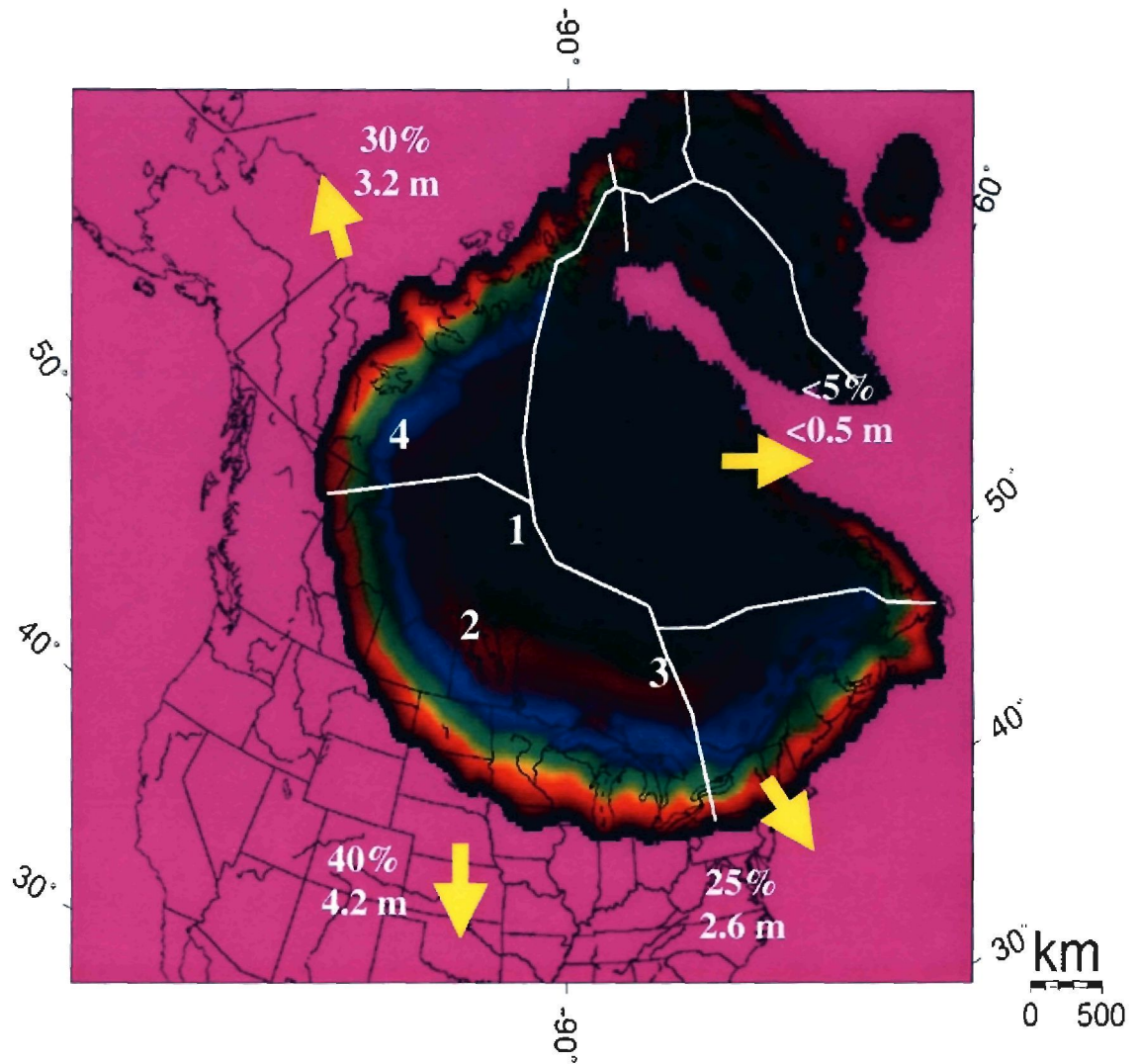


**Fig. 28.** Thickness difference between -15,000 and -14,600 model years. Bright hues indicate maximum change. The most volume loss occurred over the southern sector of the LIS. Negligible loss occurred over the Hudson Bay region and the GIS, as illustrated by dark hues. Approximate volume contributions of each drainage zone is listed next to arrows indicating meltwater pathways.

## 6. CONCLUSIONS

- MWP 1A is commonly inferred to have encompassed a dramatic rise in sea-level of 13.5 – 24 m in 300 – 1000 years; however, a review of basic data indicates that there is little evidence firmly establishing either magnitude or timing of the event. The sea-level jump was originally postulated to explain a hiatus between two drill cores obtained from a coral reef (Fairbanks 1989). A single core with a complete record of the meltwater pulse was not recovered. Similarly, a more recent study (Hanebuth 2003) provided ample data; unfortunately, the record is contaminated with radiocarbon age reversals. Thus, there is doubt as to the magnitude of MWP 1A and whether or not the event actually occurred.
- If real, MWP 1A could have originated from the LIS. Sea-water freshening during the time of MWP 1A *ca.* 14,000 calendar years B.P. is evident in marine sediment cores retrieved from the Gulf of Mexico and Bermuda Rise. This indicates that the southern margin of the LIS was a likely source. However, that sector of the ice sheet was probably too thin to yield enough freshwater for a pulse the magnitude of MWP 1A (Clark *et al.* 1996).
- Alternatively, it was suggested that MWP 1A originated from Antarctica (Clark *et al.* 1996; Weaver *et al.* 2003). Because the AIS lacks a surface melt zone, a mechanical collapse is required to produce a meltwater pulse. One possible mechanism is that of exploding ice shelves (*e.g.*, Scambos 2000), whereby shelf disintegration facilitates the acceleration of ice streams and rapid drainage of interior ice. However, there is a caveat to citing Antarctica as the source of MWP

1A. Two-thirds of the 14 m (s.l. equiv.) additional LGM ice volume in Antarctica was contained in the West Antarctic Ice Sheet (Denton and Hughes 2002). Glacial recession began in the Ross Sea embayment, West Antarctica during mid to late-Holocene time (Conway *et al.* 1999; Hall and Denton 2000). Thus, the known deglacial chronology and total ice volume availability is incompatible with MWP 1A originating from Antarctica *ca.* 14,000 calendar years B.P.

- The UMISM generated an unrealistic LIS that engulfed North America in simulations wherein the GISP2 ice-core record (with a 23 °C LGM mean-annual temperature depression) was used to drive model climate. A reasonable ice sheet reconstruction was possible by scaling down the GISP2 temperature signal significantly (LGM temperature depression <10 °C); however, it was not possible to attain a realistic glacial termination.
- A correct LGM configuration and initial deglaciation was attained for the LIS by using the EPICA Dome C ice core record to drive model climate. The modest warm peak in EPICA preceding the ACR was not enough to produce a freshwater pulse. It was necessary to impose an artificial warming on the ice sheet in order for the model to generate a meltwater pulse of significant magnitude. Even then, only the most extreme scenario, whereby a modern climate regime was sustained for 300 years, affords values (10.5 m sea-level jump in 500 years) that barely fall within the lower acceptable limit of MWP 1A.
- Overall, this study places a question on the validity of MWP 1A.



## REFERENCES

- Anderson, J. B. and Andrews, J. T., 1999: Radiocarbon constraints on ice sheet advance and retreat in the Weddell Sea, Antarctica. *Geology*, 27, 2: 179-182.
- Andrews, J. T., Erlenkeuser, H., Tedesco, K., Aksu, A. E. and Jull, A. J. T., 1994: Late Quaternary (stage 2 and 3) meltwater and Heinrich events, northwest Labrador Sea. *Quaternary Research*, 41: 26-34.
- Atkinson, T. C., Briffa, K. R. and Coope, G. R., 1987: Seasonal temperatures in Britain during the past 22,000 years, reconstructed using beetle remains. *Nature*, 325: 587-592.
- Bard, E., Hamelin, B., Fairbanks, R. G. and Zindler, A., 1990: Calibration of the  $^{14}\text{C}$  timescale over the past 30,000 years using mass spectrometric U-Th ages from Barbados corals. *Nature*, 345: 405-410.
- Bard, E., Hamelin, B., Arnold, M., Montaggioni, L., Cabioch, G., Faure, G. and Rougerie, F., 1996: Deglacial sea-level record from Tahiti corals and the timing of global meltwater discharge. *Nature*, 382: 241-244.
- Baumgartner, A. and Reichel, E., 1975: *The World Water Balance*. Elsevier, New York.
- Bentley, M. J. and Anderson, J. B., 1998: Glacial and marine geological evidence for the ice sheet configuration in the Weddell Sea-Antarctic Peninsula region during the Last Glacial Maximum. *Antarctic Science*, 10: 309-325.
- Blanchon, P. and Shaw, J., 1995: Reef drowning during the last glaciation: evidence for catastrophic sea-level rise and ice sheet collapse. *Geology*, 23, 1: 4-8.
- Blunier, T., Chappellaz, J., Schwander, J., Dallenbach, A., Stauffer, B., Stocker, B., Raynaud, D., Jouzel, J., Clausen, H., Hammer, C. and Johnsen, S., 1998: Asynchrony of Antarctic and Greenland climate change during the last glacial period. *Nature*, 394: 739-743.
- Blunier, T. and Brook, E. J., 2001: Timing of millennial-scale climate change in Antarctica and Greenland during the last glacial period. *Science*, 291: 109-112.
- Bond, G., Heinrich, H., Huon, S., Broecker, W., Labeyrie, L., Andrews, J., McManus, J., Clasen, S., Tedesco, K., Jantschik, R., Simet, C. and Klas, M., 1992: Evidence for massive discharges of icebergs into the glacial Northern Atlantic. *Nature*, 360: 245-249.



- Borns, H. W., Jr., Dorian, C. C., Jacobson, G. L., Jr., Kreutz, K. J., Thompson, W. B., Weddle, T. K., Doner, L. A., Kaplan, M. R. and Lowell, T. V., 2003 in press, The deglaciation of Maine. *INQUA commission on glaciation*.
- Braithwaite, R. J. and Olesen, O. B., 1989: Calculation of glacier ablation from air temperature, West Greenland. *Glacier Fluctuations and Climate Change*, Dordrecht, Kluwer Academic Publishers: 219-233.
- Brockheim, J. G., Wilson, S. C., Denton, G. H., Andersen, B. G. and Stuiver, M., 1989: Late Quaternary ice-surface fluctuations of Hatherton Glacier, Transantarctic Mountains. *Quaternary Research*, 31: 229-254.
- Buddemeier, R. W. and Smith, S. V., 1988: Coral reef growth in an era of rapidly rising sea level: Predictions and suggestions for long-term research. *Coral Reefs*, 7: 51-56.
- Chappell, J. and Polach, H., 1991: Postglacial sea-level rise from a coral record at Huon Peninsula, Papua New Guinea. *Nature*, 349: 147-149.
- Clark, P. U., Alley, R. B., Keigwin, L. D., Licciardi, J. M., Johnsen, S. J. and Wang, H., 1996: Origin of the first global meltwater pulse following the last glacial maximum. *Paleoceanography*, 11, 5: 563-577.
- Cuffey, K. M. and Clow, G. D. 1997: Temperature, accumulation, and ice sheet elevation in central Greenland through the last deglacial transition. *Journal of Geophysical Research*, 102: 26,383-26,396.
- Denton, G. H., Bockheim, J. G., Wilson, S. C. and Stuiver, M., 1989a: Late Wisconsin and early Holocene glacial history, inner Ross Embayment, Antarctica. *Quaternary Research*, 31: 151-182.
- Denton, G. H., Bockheim, J. G., Wilson, S. C., Leide, J. E. and Andersen, B. G., 1989b: Late Quaternary ice-surface fluctuations of Beardmore Glacier, Transantarctic Mountains. *Quaternary Research*, 31: 183-209.
- Denton, G. H. and Hughes, T. J., 2000: Reconstruction of the Ross ice drainage system, Antarctica, at the last glacial maximum. *Geografiska Annaler*, 82 A: 143-166.
- Denton, G. H. and Hughes, T. J., 2002: Reconstructing the Antarctic ice sheet at the last glacial maximum. *Quaternary Science Reviews*, 21: 193-202.
- Edwards, R. L., Beck, J. W., Burr, G. S., Donahue, D. J., Chappell, J. M. A., Bloom, A. L., Druffel, E. R. M. and Taylor, F. W., 1993: A large drop in atmospheric  $^{14}\text{C}/^{12}\text{C}$  and reduced melting in the Younger Dryas, documented with  $^{230}\text{Th}$  ages of corals. *Science*, 260: 962-968.

- Fairbanks, R. G. and Matthews, R. K., 1978: The marine oxygen isotope record in Pleistocene coral, Barbados, West Indies. *Quaternary Research*, 10: 181-196.
- Fairbanks, R. G., 1989: A 17,000-year glacio-eustatic sea level record: influence of glacial melting rates on the Younger Dryas event and deep-ocean circulation: *Nature*, 342: 637-642.
- Fastook, J. L. and Prentice, M., 1994: A finite-element model of Antarctica: sensitivity test for meteorological mass-balance relationship. *Journal of Glaciology*, 40, 134: 167-175.
- Fastook, J. L., 2002: University of Maine Ice Sheet Model. Unpublished.
- Fortuin, I. P. F. and Oerlemans, J., 1990: Parameterization of the annual surface temperature and mass balance of Antarctica. *Annals of Glaciology*, 14: 78-84.
- Goodwin, I. D., 1993: Holocene deglaciation, sea-level change, and the emergence of the Windmill Islands, Budd Coast, Antarctica. *Quaternary Research*, 40: 70-80.
- Goreau, T. F., 1959: The ecology of Jamaican coral reefs. I. Species composition and zonation: *Ecology*, 40: 67-90.
- Guilderson, T. P., Fairbanks, R. G. and Rubenstone, J. L., 2001: Tropical Atlantic coral oxygen isotopes: glacial-interglacial sea surface temperatures and climate change. *Marine Geology*, 172: 75-89.
- Hall, B. L. and Denton, G. H., 2000: Radiocarbon chronology of Ross Sea Drift, eastern Taylor Valley, Antarctica: evidence for a grounded ice sheet in the Ross Sea at the last glacial maximum. *Geografiska Annaler*, 82 A: 305-336.
- Hanebuth, T., Stattegger, K. and Grootes, P. M., 2000: Rapid flooding of the Sunda Shelf: a late-glacial sea-level record. *Science*, 288: 1033-1035.
- Huybrechts, P., 2002: Sea-level changes at the LGM from ice-dynamic reconstructions of the Greenland and Antarctic ice sheets during the glacial cycles. *Quaternary Science Reviews*, 21: 203-231.
- Johnsen, S.J., Clausen, H.B., Dansgaard, W., Gundestrup, N.S., Hammer, C.U., Andersen, U., Andersen, K.K., Hvidberg, C.S., DahlJensen, D., Steffensen, J.P., Shoji, H., Sveinbjornsdottir, A.E., White, J., Jouzel, J. and Fisher, D., 1997: The delta O-18 record along the Greenland Ice Core Project deep ice core and the problem of possible Eemian climatic instability. *Journal of Geophysical Research*, 102: 26397-26410.

- Jouzel, J. and Merlivat, L., 1984: Deuterium and oxygen 18 in precipitation: modeling of the isotopic effects during snow formation. *Journal of Geophysical Research*, 89: 11,749-11,757.
- Keigwin, L. D., Jones, G. A., Lehman, S. J. and Boyle, E. A., 1991: Deglacial meltwater discharge, North Atlantic deep circulation, and abrupt climate change. *Journal of Geophysical Research*, 96: 16,811-16,826.
- Keigwin, L. D. and Jones, G. A., 1995: The marine record of deglaciation from the continental margin off Nova Scotia. *Paleoceanography*, 10: 973-985.
- Leventer, A., Williams, D. F. and Kennett, J. P., 1982: Dynamics of the Laurentide Ice Sheet during the last glaciation: Evidence from the Gulf of Mexico. *Earth and Planetary Science Letters*, 59: 11-17.
- Licht, K. J., Jennings, A. E., Andrews, J. T. and Williams, K. M., 1996: Chronology of late Wisconsin ice retreat from the western Ross Sea, Antarctica: *Geology*, 24, 3: 223-226.
- Licht, K. J., Dunbar, N. W., Andrews, J. T. and Jennings, A. E., 1999: Distinguishing subglacial till and glacial marine diamictos in the western Ross Sea, Antarctica: Implications for a last glacial maximum grounding line. *GSA Bulletin*, 111, 1: 91-103.
- Lowe, A. L. and Anderson, J. B., 2002: Reconstruction of the West Antarctic ice sheet in Pine Island Bay during the Last Glacial Maximum and its subsequent retreat history. *Quaternary Science Reviews*, 21: 1879-1897.
- Lundqvist, J. and Saarnisto, M., 1995: Summary of Project IGCP-253: *Quaternary International*, 28: 9-18.
- Miura, H., Moriwaki, K., Maemoku, H. and Hirakawa, K., 1998: Fluctuations of the East Antarctic ice-sheet margin since the last glaciation from the stratigraphy of raised beach deposits along the Soya Coast. *Annals of Glaciology*, 27: 297-301.
- Morgan, V., Delmotte, M., Ommen, T. van, Jouzel, J., Chappellaz, J., Woon, Suenor, Masson-Delmotte, V. and Raynaud, D., 2002: Relative timing of deglacial climate events in Antarctica and Greenland. *Science*, 297: 1862-1864.
- Peixoto, J. P. and Oort, A. H., 1992: *Physics of Climate*. Springer-Verlag New York, Inc.
- Peltier, W. R., 1994: Paleotopography of glacial-age ice sheets. *Science*, 265: 195-201.

- Petit, J. R., Jouzel, J., Raynaud, D., Barkov, N.I., Barnola, J. M., Basile, I., Bender, M., Chappellaz, J., Davis, M., Delaygue, G., Delmotte, M., Kotlyakov, V. M., Legrand, M., Lipenkov, V. Y., Lorius, C., Pepin, L., Ritz, C., Saltzman, E. and Stievenard, M., 1999: Climate and atmospheric history of the past 420,000 years from the Vostok ice core, Antarctica. *Nature*, 399: 429-436.
- Scambos, T., Hulbe, C., Fahnestock, M. and Bohlander, J., 2000: The link between climate warming and break-up of ice shelves in the Antarctic Peninsula. *Journal of Glaciology*, 46: 516-530.
- Schwander, J., Jouzel, J., Hammer, C. U., Petit, J., R., Udisti, R. and Wolff, E., 2001: A tentative chronology for the EPICA Dome Concordia ice core, *Geophysical Research Letters*, 28, 22: 4243-4246.
- Schwerdtfeger, W., 1984: *Weather and Climate of the Antarctic: Developments in Atmospheric Science I*. Amsterdam and New York, Elsevier.
- Severinghaus, J. P., Sowers, T., Brook, E. J., Alley, R. B. and Bender, M. L., 1998: Timing of abrupt climate change at the end of the Younger Dryas interval from thermally fractionated gases in polar ice. *Nature*, 391: 141-146.
- Shackleton, N. J., 1987: Oxygen isotopes, ice volume and sea level. *Quaternary Science Reviews*, 6: 183-190.
- Shipp, S., Anderson, J. and Domack, E., 1999: Late Pleistocene Holocene retreat of the west Antarctic ice-sheet system in the Ross Seas: Part I—geophysical results. *GSA Bulletin*, 111: 1486-1516.
- Siddall, M., Rohling, E. J., Almogi-Labin, A., Hemleben, C., Meischner, D., Schmelzer, I. and Smeed, D. A., 2003: Sea-level fluctuations during the last glacial cycle. *Nature*, 423: 583-588.
- Weaver, A. J., Saenko, O. A., Clark, P. U. and Mitrovica, J. X., 2003: Meltwater Pulse 1A from Antarctica as a trigger of the Bølling-Allerød warm interval. *Science*, 229: 1709-1713.
- Yokoyama, Y., Lambeck, K., de Dekhar, P., Johnston, P. and Fifield, L. K., 2000: Timing of the Last Glacial Maximum from observed sea level minima. *Nature*, 406: 713-716.

## APPENDIX A

### *University of Maine Ice Sheet Model Description*

The University of Maine Ice Sheet Model (UMISM) (Fastook 2002) is a multi-component map-plane glaciological model that uses the finite-element numerical technique to solve conservation equations – mass and momentum conservation for ice dynamics, and energy conservation for internal temperatures. Other components include: 1) hydrostatically supported visco-elastic plate model for bed depression and rebound; 2) basal water module; 3) simple climatology model for surface temperatures and mass balance. The UMISM is capable of deriving both steady-state, and time-dependent solutions.

A chronological record of paleo-temperature is required as input to the UMISM for time-dependent ice sheet reconstruction. Such a record provides a climate baseline, or the temperature that is felt at a defined location at sea-level. This baseline is used by the embedded simple climatology model (Fastook and Prentice 1994) to facilitate the parameterization of the effects of an ice sheet on local climate. Input temperatures are departures from present. For instance, an input of 0 °C indicates a mean modern climate. A higher value would afford generation of a warmer climate and conversely a negative value would result in a colder climate. The model calculates a temperature spectrum from the sea-level base to the pole using horizontal (latitude) and vertical (elevation) lapse rates. Precipitation, ablation and a net mass balance at each node in the model map-plane is then determined using a meteorological scheme developed by (Fastook and

Prentice 1994) (*see Appendix 2*).

Bedrock topography is a fundamental input. Because relief under an ice sheet can greatly affect ice dynamics, particularly with respect to the position and growth of ice streams, it is important to have a high resolution digital terrain grid. The topographic dataset used with the UMISM was ETOPO5, a 5-minute grid developed by the U.S. Geological Survey.

Model parameters can be adjusted after the UMISM is supplied with bedrock topography and temperature datasets. One option is to establish different meteorological zones within a given simulation map-plane in order to create realistic climate. The simple climatology model is not a Global Circulation Model (GCM). It is incapable of considering the important effects of heat advection due to atmospheric and oceanic circulation. For example, the UMISM does not differentiate between polar and sub-tropical air masses. Assigning individual climatic zones (that can use separate mass-balance schemes) affords a way to bypass the inherent limitations of the simple climatology model.

The position of the pole can be changed in the model. Changing the pole position is synonymous with changing the center point of meteorological calculations. The influence of this parameter has an important effect on ice sheet growth. A pole setting of precisely 90 °N latitude affords an unrealistic ice sheet that spreads predominantly over the North American Cordilleran and lowlands of western Canada. I found that an optimal LIS reconstruction could be attained with the pole located over southern Greenland (66 °N, 45 °W). This setting was used for all simulations reported here.

Grounding-line calving and ice hardness are other important adjustable parameters. The calving parameter is a multiplier to the calving rate. A positive value will augment whereas a negative value will diminish marginal ablation. Adjustments to the ice hardness parameter (flow enhancement factor) change the physical ability of the ice to resist internal shear. “Hard” ice leads to high domes, whereas “soft” ice facilitates the growth of comparatively low domes. Hardness, dependent upon temperature, is calculated from the ice flow law. A flow enhancement factor is added to ice hardness to accommodate observed differences between the Greenland and Antarctic ice sheets. The LIS is assumed to have had a similar value to that of Greenland Ice Sheet (Fastook pers. comm.).

## APPENDIX B

### *Mass-Balance Calculations*

In order to generate time-dependent solutions, the UMISM uses an embedded simple climatology module that calculates accumulation and ablation based on a mean-annual temperature input. The mass-balance scheme is derived from an empirical fit to present accumulation rates over the Antarctic continent (Jouzel and Merlivat 1984; Fortuin and Oerelmans 1990). This relationship depends on surface elevation, surface slope and latitude. Ablation rates are based upon mass-balance data from West Greenland (Braithwaite and Olesen 1989). The simple climatology is driven by a mean-annual temperature input. This input is used in the meteorological equations described below. A net mass-balance for each node in the map-plane is then determined and used as input for the glaciological model.

First, a mean annual surface temperature ( $T_S$ , units °C) is calculated based on lapse rates and distance to the pole.

$$T_S = A_L h + B_L L_{AT} + T_{climate} + T_{input}$$

Where  $A_L$  and  $B_L$  are vertical (wet adiabatic, -6 °C/km) and horizontal (0.55 °C/° latitude) lapse rates respectively,  $h$  is surface elevation,  $L_{AT}$  is latitude, and  $T_{climate}$  is a climate knob. The climate knob is used to calibrate the model to a present-day mean-annual temperature at a specific spot on earth.  $T_{input}$  is the mean-annual temperature input supplied to the model.



Next, a standard meteorological relationship is used to obtain a free atmosphere-thermal layer temperature ( $T_F$ , units K).

$$T_F = 0.67(T_S + 273.0) + 88.9$$

A saturation vapor pressure over ice ( $E_{Si}$ , units mbar) is then calculated using the Goff-Gratch equation.

$$E_{Si} = 10^X$$

Where  $X$  is a standard meteorological solution.

The accumulation rate ( $A_{ACC}$ , units m/yr) is then calculated by fitting accumulation rate as a function of saturation vapor pressure and surface slope ( $X_{SLOPE}$ ; units m/km).

$$A_{ACC} = WE_S + X_{SLOPE} + Z$$

Based on assumptions of seasonality being a function of latitude and month, the number of positive degree days is calculated to model ablation. The seasonality factor represents incoming solar radiation at the top of the atmosphere. A latitudinal slope ( $QS_1$ , units  $\text{ly d}^{-1} \text{ }^\circ \text{ lat}^{-1}$ ) and intercept ( $QSI$ , units  $\text{ly d}^{-1}$ ) is then obtained from published values (Sellers 1965). From this, an annual mean can be calculated.

$$QY = 1/12 \sum_{I=1}^{12} (QI_I - QS_I L_{AT})$$

A monthly mean temperature is then calculated by taking the mean annual temperature as a function of the difference between the annual mean and the monthly solar radiations. A proportionality constant is then obtained from station data (Schwerdtfeger 1984).

$$T_I = T_S + 0.021((QI_I - QS_I L_{AT}) - QY)$$

The ablation rate is calculated by using the annual sum of positive degree days.

$$P_{DD} = \sum_{I=1}^{12} 30T_I$$

$$A_{BL} = 0.006P_{DD}$$

$P_{DD}$  is multiplied by a proportionality constant obtained from West Greenland ablation data (Braithwaite and Olesen 1989). A net mass-balance ( $a_{DOT}$ , units m/yr) is finally calculated by subtracting ablation from accumulation.

$$a_{DOT} = A_{CC} - A_{BL}$$

## **BIOGRAPHY OF THE AUTHOR**

Sean D. Birkel was born in Bangor, ME in 1978. He graduated from Bangor High School in Bangor, Maine in 1996. Sean entered the University of Maine in September of 1997 to pursue a Bachelor of Science degree in Geological Sciences. After graduating in May, 2002, he entered the Graduate School. Sean worked as a field assistant in the Dry Valleys, Antarctica for Dr. Brenda L. Hall during the 2002-2003 season. Sean is a candidate for the Master of Science degree in Quaternary and Climate Studies from The University of Maine in December, 2004.